AD-A115 170 COMPUTER SCIENCES CORP ALBUQUERQUE NM F/G 9/1
200 KJ COPPER FOIL FUSES.(U)
APR 80 C R MCCLENAHAN, J H GOFORTH F29601-78-C-0012
UNCLASSIFIED AFWL-TR-78-130 NL

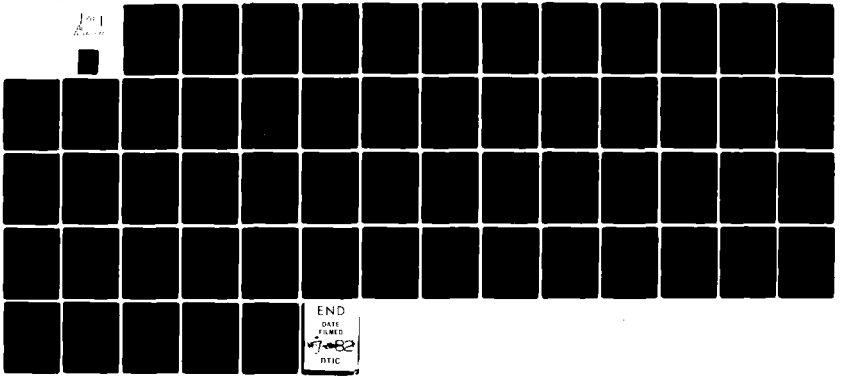

END
DATE FILMED
7-82
DTIC

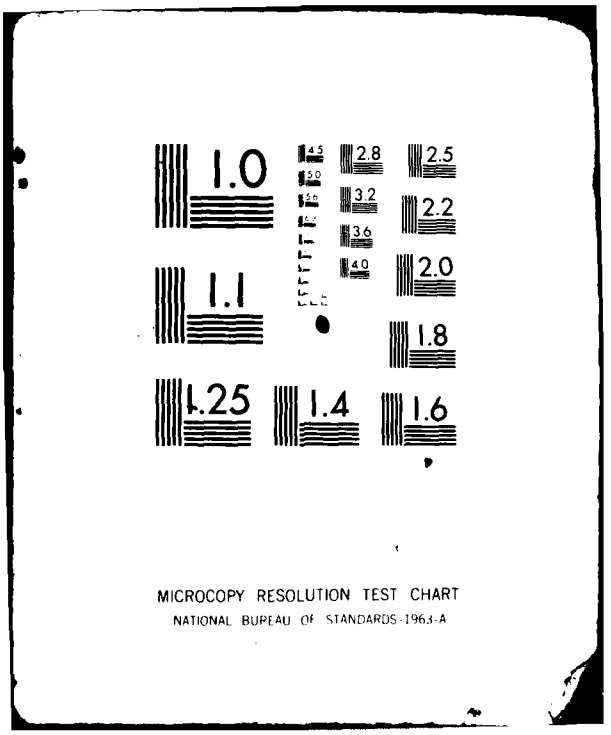
1.0
1.1
1.25
1.4
1.6
1.8
2.0
2.2
2.5
2.8
3.2
3.6
4.0
4.5
5.0
MICROCOPY RESOLUTION TEST CHART
NATIONAL BUREAU OF STANDARDS-1963-A

AFWL-TR-78-130

(2)

AFWL-TR-
78-130

200 kJ COPPER FOIL FUSES

C. R. McClenahan, et al.

Computer Sciences Corporation
1400 San Mateo Blvd. S.E.
Albuquerque, NM 87108

April 1980

Final Report

AIR FORCE WEAPONS LABORATORY
Air Force Systems Command
Kirtland Air Force Base, NM 87117

AFWL-TR-78-130

This final report was prepared by Computer Sciences Corporation, Albuquerque, New Mexico, under Contract F29601-78-C-0012, Job Order ILIR7608 with the Air Force Weapons Laboratory, Kirtland Air Force Base, New Mexico. Captain Charles R. McClenahan (NTYP) was the Laboratory Project Officer-in-Charge.

When US Government drawings, specifications, or other data are used for any purpose other than a definitely related Government procurement operation, the Government thereby incurs no responsibility nor any obligation whatsoever, and the fact that the Government may have formulated, furnished, or in any way supplied the said drawings, specifications, or other data, is not to be regarded by implication or otherwise, as in any manner licensing the holder or any other person or corporation, or conveying any rights or permission to manufacture, use, or sell any patented invention that may in any way be related thereto.

This report has been authored by a contractor of the United States Government. The United States Government retains a nonexclusive, royalty-free license to publish or reproduce the material contained herein, or allow others to do so, for the United States Government purposes.

This report has been reviewed by the Public Affairs Office and is releasable to the National Technical Information Service (NTIS). At NTIS, it will be available to the general public, including foreign nations.

This technical report has been reviewed and is approved for publication.

James H. Degnan

JAMES H. DEGNAN, PhD
Project Officer

FOR THE DIRECTOR

Norman F. Roderick

NORMAN F. RODERICK
Lt Colonel, USAF
Chief, Advanced Concepts Branch

Thomas W. Ciambrone

THOMAS W. CIAMBRONE
Colonel, USAF
Chief, Applied Physics Division

DO NOT RETURN THIS COPY. RETAIN OR DESTROY.

UNCLASSIFIED

SECURITY CLASSIFICATION OF THIS PAGE (When Data Entered)

REPORT DOCUMENTATION PAGE		READ INSTRUCTIONS BEFORE COMPLETING FORM
1. REPORT NUMBER AFWL-TR-78-130	2. GOVT ACCESSION NO. AD-A115170	3. RECIPIENT'S CATALOG NUMBER
4. TITLE (and Subtitle) 200 kJ COPPER FOIL FUSES		5. TYPE OF REPORT & PERIOD COVERED Final Report 6. PERFORMING ORG. REPORT NUMBER
7. AUTHOR(s) C. R. McClenahan R. M. Henderson J. H. Goforth W. H. Janssen J. H. Degnan W. E. Walton		8. CONTRACT OR GRANT NUMBER(s) F29601-78-C-0012
9. PERFORMING ORGANIZATION NAME AND ADDRESS Computer Sciences Corporation 1400 San Mateo Blvd. S.E. Albuquerque, NM 87108		10. PROGRAM ELEMENT, PROJECT, TASK AREA & WORK UNIT NUMBERS 61101F/ILIR7608
11. CONTROLLING OFFICE NAME AND ADDRESS Air Force Weapons Laboratory (NTYP) Kirtland Air Force Base, NM 87117		12. REPORT DATE April 1980 13. NUMBER OF PAGES 56
14. MONITORING AGENCY NAME & ADDRESS(if different from Controlling Office)		15. SECURITY CLASS. (of this report) Unclassified 15a. DECLASSIFICATION/DOWNGRADING SCHEDULE

16. DISTRIBUTION STATEMENT (of this Report)

Approved for public release; distribution unlimited.

17. DISTRIBUTION STATEMENT (of the abstract entered in Block 20, if different from Report)

18. SUPPLEMENTARY NOTES

19. KEY WORDS (Continue on reverse side if necessary and identify by block number)

Inductive Energy Storage
Opening Switch
Copper Foil Fuse
Glass Beads
Maisonnier Criteria

20. ABSTRACT (Continue on reverse side if necessary and identify by block number)

A 200-kJ, 50-kV capacitor bank has been discharged into 1-mil-thick copper foils immersed in fine glass beads. These foils ranged in length from 27 to 71 cm and in width from 15 to 40 cm. Voltage spikes of over 250 kV were produced by the resulting fuse behavior of the foil. Moreover, the current turned off at a rate that was over 6 times the initial bank dI/dt. Full widths at half maxima for the voltage and dI/dt spikes were about 0.5 us, with some as short as 300 ns. Electrical breakdown was prevented in all but one size fuse with maximum applied

DD FORM 1 JAN 73 1473

UNCLASSIFIED

SECURITY CLASSIFICATION OF THIS PAGE (When Data Entered)

20. ABSTRACT

fields of 7 kV/cm. Fuses that were split into two parallel sections have been tested, and the effects relative to one-piece fuses are much larger than would be expected on the basis of inductance differences alone. A resistivity model for copper foil fuses, which differs from previous work in that it includes a current density dependence, has been devised. Fuse behavior is predicted with reasonable accuracy over a wide range of foil sizes by a quasi-two-dimensional fuse code that incorporates this resistivity model. A variation of Maisonnier's method for predicting optimum fuse size has been derived. This method is valid if the risetime of the bank exceeds 3 μs, in which case it can be expected to be applicable over a wide range of peak current densities.

TABLE OF CONTENTS

ILLUSTRATIONS

Illustrations (continued)

Illustrations (continued)

SECTION I

INTRODUCTION

The use of a large, slow energy storage device to store energy in the magnetic field of an inductor and subsequently transferring a significant fraction of the stored energy to a parallel load by means of an opening and a closing switch has been suggested by several authors (references 1-4) and is illustrated in figure 1. The energy delivery time to the parallel load can be significantly shorter than the charging time for the storage inductor, resulting in energy pulse compressions of factors of 5 to 10. For a matched load (load inductance equal to storage inductance), a maximum of 25% of the initial energy in the storage inductor can be transferred to the load (reference 3). If the load is dissipative (for example, a SHIVA electromagnetic implosion, reference 5), a substantially higher fraction of the stored energy could be transferred. A fuse could serve for the opening switch, and it would be required to interrupt currents of many megamps and to hold off voltages of hundreds of kilovolts.

Using a very large capacitor bank, homopolar generator (reference 6), or explosive magnetic flux compression generator (reference 7) with one or more storage inductor/ opening switch pulse sharpening stages, extremely high energy ($\sim 10^7$ to 10^8 j) and high power ($\sim 10^{14}$ to 10^{15} w) pulses may be possible. Fuses for such pulsed power devices would interrupt $\sim$30 to 300 MA, hold off $\sim$300 kV to 3 MV, and absorb at least 10% of the stored energy without restriking.

The purpose of this work was to extend the fuse performance of copper foils achieved by Di Marco (reference 4, 800-kA, 80-kV, 25-kj) to a 2-MA, 250-kV, 200-kj operation. Also, information on the scaling of fuse behavior and resistivity (references 4 and 8) with energy was sought.

Some useful criteria for estimating optimum fuse size for a given circuit are those given by Maisonnier (reference 3). The first criterion is that the energy deposited in the fuse by I^2R heating should be just enough to initiate fuse vaporization at maximum current when the charge left stored in the capacitor bank is zero. The

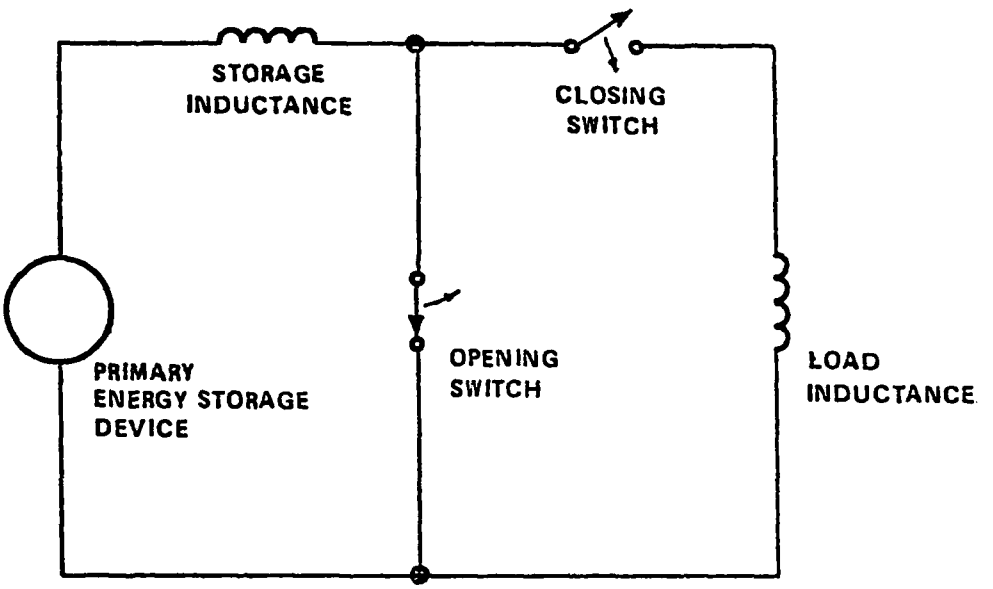

Figure 1. Schematic Diagram of Inductive Energy-Storage Circuit.

second is that the fuse mass should be such that the energy which must be dissipated in the fuse is just enough to vaporize it. These criteria result in conditions on the fuse length and cross section in terms of the bank capacitance, total inductance, initial charge on the bank, and the fuse material properties. These criteria were used as a guide for a parameter survey in this work.

SECTION II

EXPERIMENTAL APPARATUS

The experiments consisted of discharging a capacitor bank into a fuse package and measuring the discharge current and the voltage across the fuse. The capacitor bank consists of 4 modules of 16 capacitors each. Two modules are connected in parallel to form an arm, and each arm discharges through four pressurized rail gap switches in parallel. The outputs of both arms are connected in parallel to the fuse.

The measured capacitance of the bank is 158 $\pm$ 3 μF, and it is charged to 50 kV to give an initial stored energy of nearly 200 kj. Short circuit shots were fired in order to measure the inductance of the bank and transmission lines. Excluding the fuse, the system inductance is 46 $\pm$ 2 nH.

Figure 2 is a cross-sectional view of a typical fuse package. A rectangular piece of copper foil is clamped to the transmission lines at opposite ends. The foil is folded around the insulator, but it is not creased. The two halves of the foil are parallel and separated by 1.5 cm. A polyethylene envelope is taped around the foil, but the envelope does not touch the foil. Glass beads (sand) are poured into the envelope to surround the foil. Care is taken to ensure that the beads fill the space between the insulator and the foil on both sides.

"Blast-O-Lite" BT-12 glass beads, which are between 62 and 105 μ in diameter, were used. It was found that the finer BT-13 beads (44 to 88 μ) showed no difference in performance, but that the coarser BT-8 beads (149 to 210 μ) resulted in significantly longer turn-off times. Since the BT-13 beads are much more difficult to handle, the BT-12 beads were routinely used.

All of the fuses were made from one roll of rolled copper sheet. An electrolytic tough-pitch copper (alloy 110) that was nominally 1-mil thick was used. Samples of the foil were weighed, and it was found to be 21.4 mg/cm^2 thick. Therefore, the equivalent thickness of the foil is 23.9 μ.

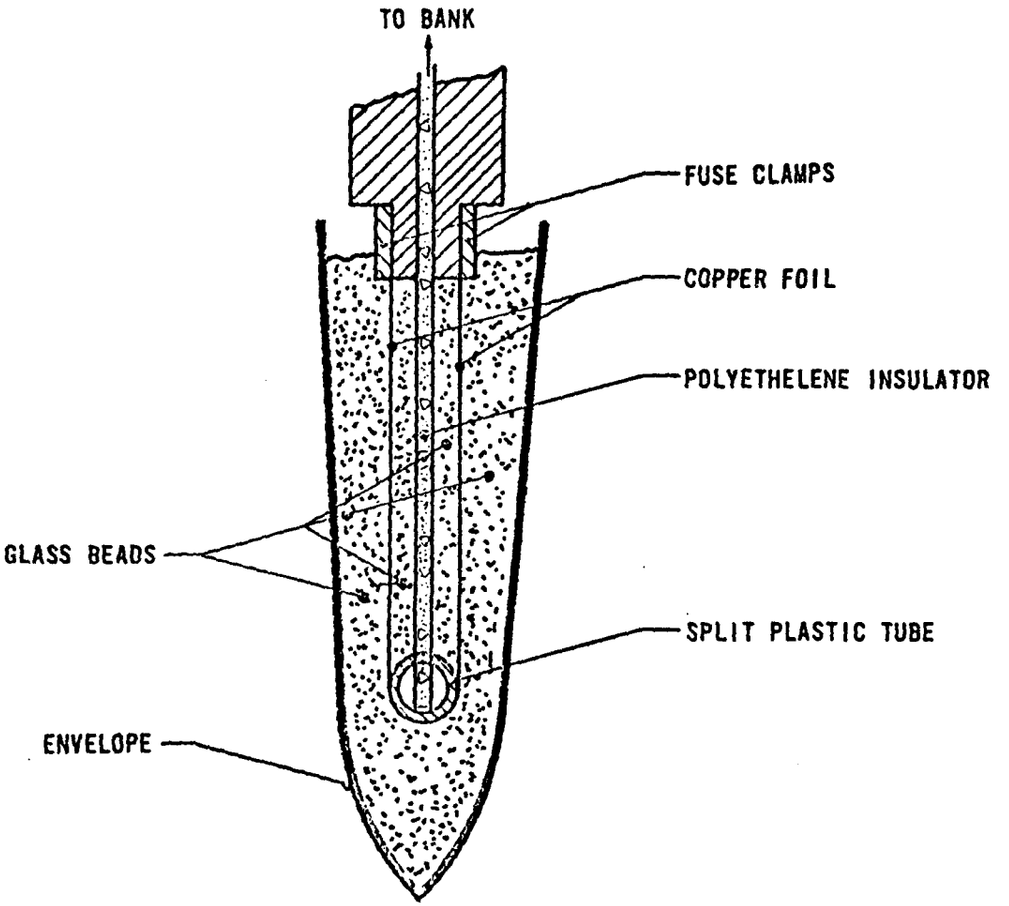

Figure 2. Cross-Sectional View of Copper Foil Fuse Package

Seventeen different fuse sizes were fired at the 200-kj level. Sizes were determined by varying the length and width. The ranges were up to $\pm$ 40% from a reference size, which was determined from Maisonnier's equations (reference 3). These equations employ three factors: k_1, k_2, and a, which are explained in reference 3. The values of these factors used in the calculation of these fuses are $k_1 = 2$, $k_2 = 1$, and $a = 5.9 \times 10^{16}$, and were obtained from Di Marco's work (reference 4).

A different reference size was calculated for each fuse inductance, since the Maisonnier size is a function of inductance. Nominal values for bank capacitance and foil thickness were used to calculate the reference sizes. The actual values were subsequently measured, and the reference sizes used are about 15% smaller than they should have been. The length of the fuses varied from 26.9 to 70.9 cm, and the width varied from 15.0 to 39.4 cm. The inductance of the fuses varied from 5.8 to 37.9 nH; however, most of the fuses had an inductance of about 14 nH.

The fuses subdivide into two classes: those where the ratio of the length to the width was constant, and those where the width was increased by the same percentage that the length was decreased. The former group had a nearly constant fuse inductance, while the latter maintained a roughly constant total fuse material.

A coil of the type normally used for Rogowski coils was used to measure the dI/dt. The coil was placed in a groove in the ground transmission plate and extended several inches past the edge of the plate. The coil was not closed as a Rogowski coil would be, but the field away from the parallel plate transmission line falls off rapidly, and the signal from the coil should be nearly the same as that from a true Rogowski coil. In any case, the coil sensitivity was measured by firing short circuit shots and recording the coil output.

A passive RC integrator was used to integrate the output of the dI/dt sensing coil, and the resulting signal was recorded on an oscillogram. The integrator employed a coaxial capacitor to give it good high-frequency response. The time constant of the integrator is 117 μs, while the foil always fused within 7 μs after the bank was fired.

Fuse voltage was measured by placing a copper sulfate water resistor across the fuse, and measuring the current through the resistor with a Tektronix CT-2 current transformer. This was taken to be proportional to the voltage across the resistor. The resistance of the water resistor was measured in two ways. A low voltage 1-kHz AC impedance bridge (General Radio model 1608) was used. Also, a 200-V, 1-μs pulse from a 2D-21 thyratron discharge was applied across the resistor. When the resistor was new, these two agreed to within the limits of the measurements ($\sim$ 5%). As the resistor aged, it developed bubbles, which were replaced with deionized water. This did not seem to effect the resistance very much as measured using the fast pulses. Over a period of about 1 year, the resistance increased by about 10%. However, the low frequency resistance (1-kHz) increased by over 100%. Therefore, the high frequency resistance was measured regularly during the experiments. Moreover, the first fuse size that was fired in a given set of experiments was repeated at the end of the experiments. No significant difference was detected in the voltage magnitude.

The frequency response of the voltage probe can be assessed by observing the rise of the fast discharge used to calibrate it. The risetime of the pulse from the thyratron tube was less than 30 ns, and the risetime of the probe output pulse was also less than 30 ns. No attempt was made to measure the frequency response more accurately.

Both current and voltage were recorded as functions of time on oscilloscopes. In addition, one oscilloscope had the current signal applied to the vertical input, and the voltage signal applied to the external horizontal input. Delays were introduced into the signals to ensure that simultaneous signals on the input cables reached their respective deflection plates on the cathode-ray tube simultaneously (within 2 ns). This gave a convenient way to define the relative positions of the current and voltage pulses. Since the signals are changing very rapidly when the foil fuses, it is important to know the relative timing accurately.

SECTION III

EXPERIMENTAL RESULTS

Figure 3 shows oscillograms of the data taken when a nominal Maisonnier-size fuse (46.6-cm-long by 27.1-cm-wide) was fired. The top trace is the voltage, and the bottom is the current. The peak voltage of about 210 kV occurred at about 4.4 μs into the discharge. A maximum of about 1.7 MA was flowing through the fuse at 3.4 μs.

The data were digitized by reading the oscillograms on a digitizing machine. Primary analysis was then carried out using the CDC 6600 computers at the Air Force Weapons Laboratory.

Figures 4 and 5 show voltage and current data for representative fuses of the constant inductance family. While the inductance changes only from 13 to 15 nH, the mass of copper changes from 9.7 to 53.0 g. Since the inductance is nearly the same, it is not surprising that the initial voltage is nearly the same for all the fuses. Moreover, the current is nearly the same until the fuse resistance increases, causing the current to shut off. It is also not surprising that the larger mass foils fuse later and at higher currents.

Figures 6 and 7 show the performance of fuses that have nearly the same foil mass but very different inductances. The inductances vary from 6 to 38 nH, but the mass varies only from 22.7 to 27.0 g. The nominal Maisonnier size fuse (46.6-cm-long by 27.1-cm-wide) has the largest mass, and the two extreme foils (26.9-cm-long by 39.4-cm-wide and 70.9-cm-long by 15.0-cm-wide) have the smallest mass. It is clear that the inductance of the fuse plays a significant roll in the initial fuse voltage and bank dI/dt. For these fuses, the smaller the cross-sectional area, the earlier it fuses.

Both families shown the peak voltage decreasing as the cross-sectional area of the fuse increases, except, in each case, for the narrowest fuse. Figure 8

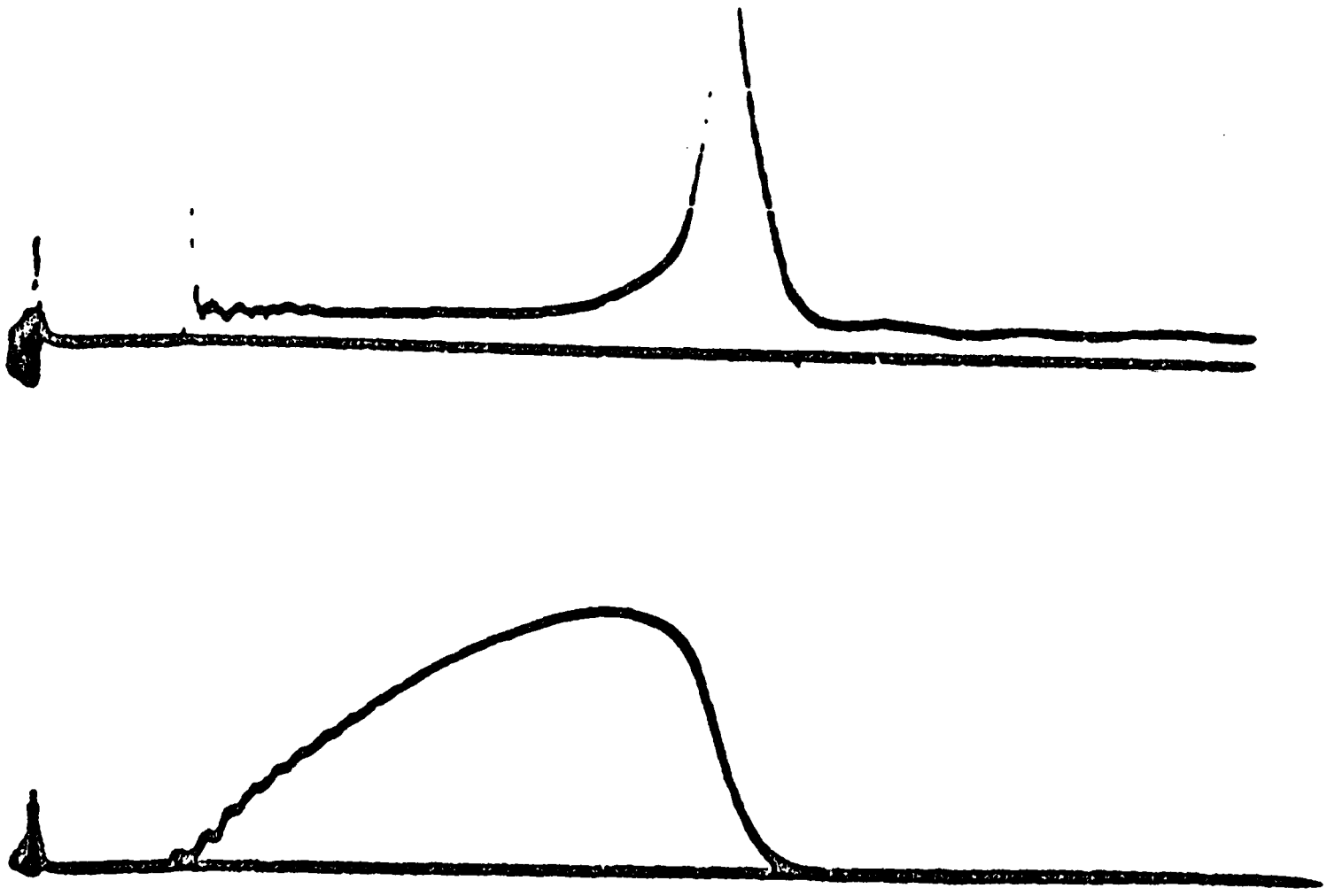

Figure 3. Oscillograms of Voltage and Current Signals for a 46.6-Cm-Long, 27.1-Cm-Wide Copper Foil Fuse. (Peak voltage of about 210 kV occurs 4.4 μs into the discharge. Peak Current of 1.66 MA is at about 3.4 μs.)

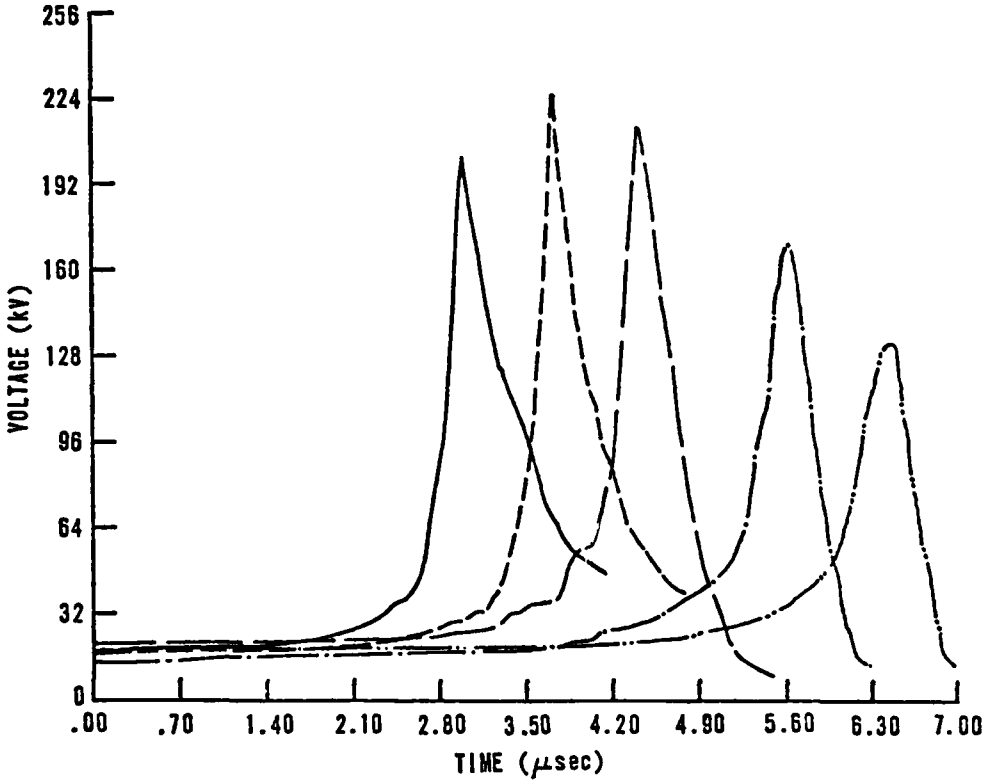

Figure 4. Voltage Data for Approximately 14-nH Copper Foil Fuses. (Solid: 27.9 cm long by 16.3 cm wide; dashed: 37.2 cm long by 21.7 cm wide; long dash: 46.6 cm long by 27.1 cm wide; dot-dash: 55.9 cm long by 32.5 cm wide; and double dot-dash: 65.2 cm long by 38.0 cm wide.)

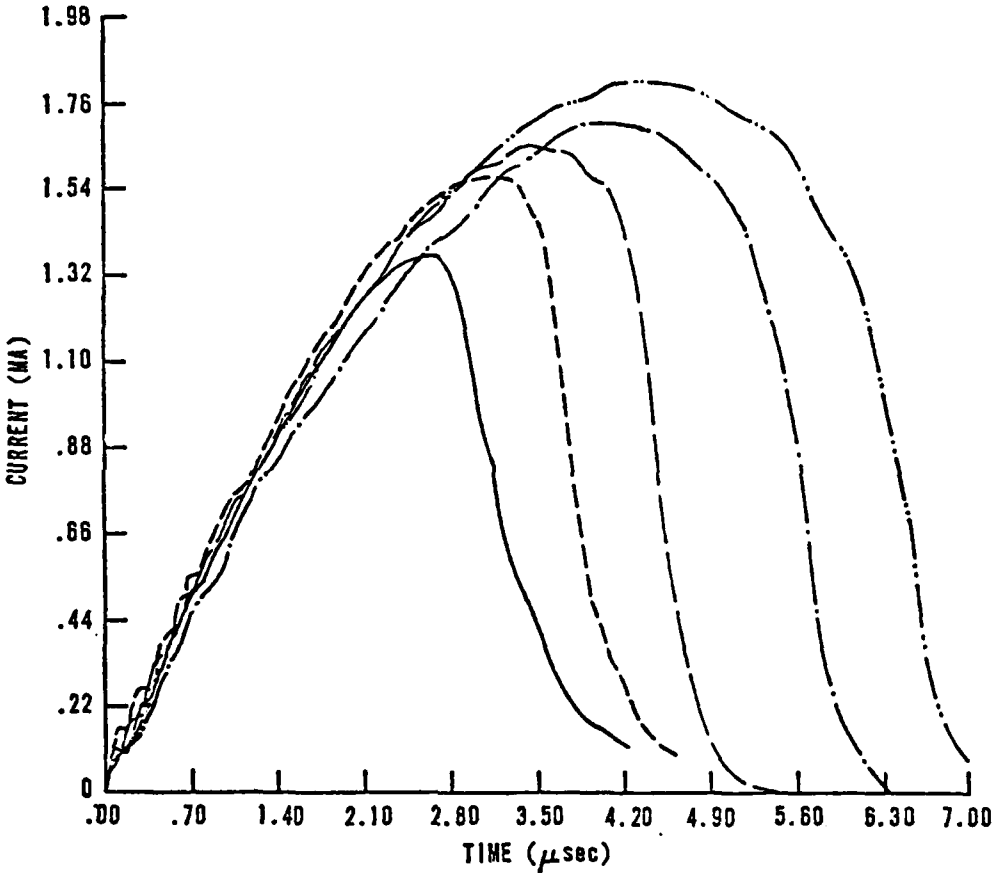

Figure 5. Current Data for Approximately 14-nH Copper Foil Fuses. (Same sizes as for figure 4.)

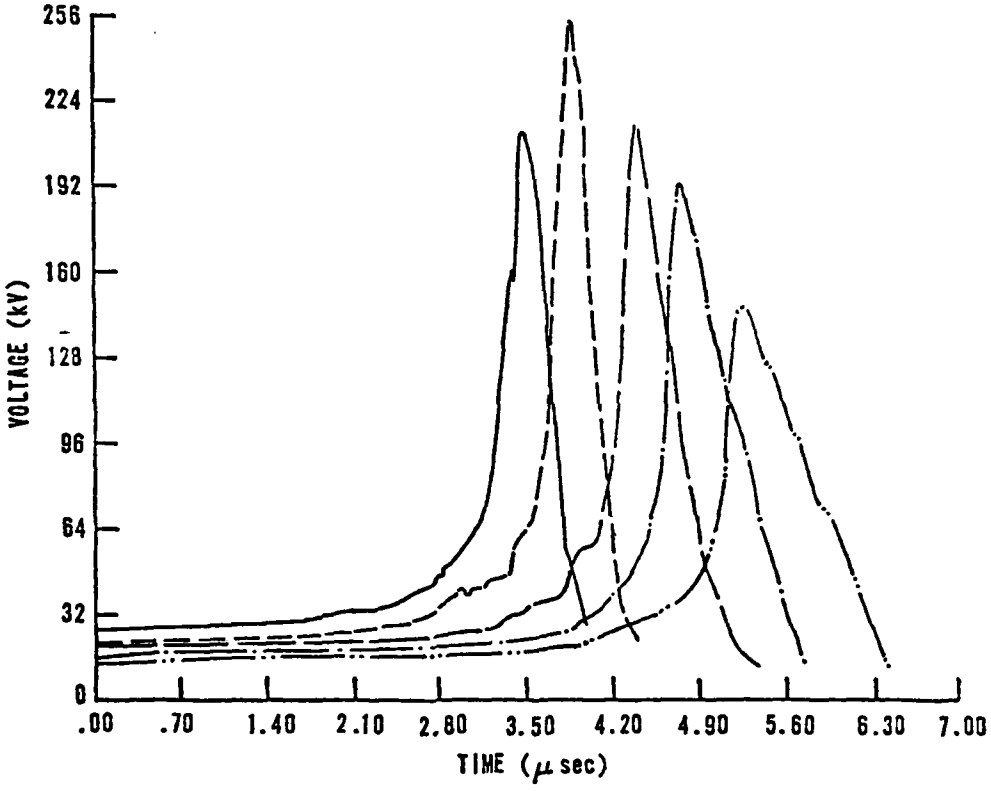

Figure 6. Voltage Data for Approximately 25-g Copper Foil Fuses. (Solid: 70.9 cm long by 15.0 cm wide; dashed: 57.7 cm long by 21.0 cm wide; long dash: 4.6 cm long by 27.1 cm wide; dot-dash: 36.5 cm long by 33.2 cm wide; and double dot-dash: 26.9 cm long by 39.4 cm wide.)

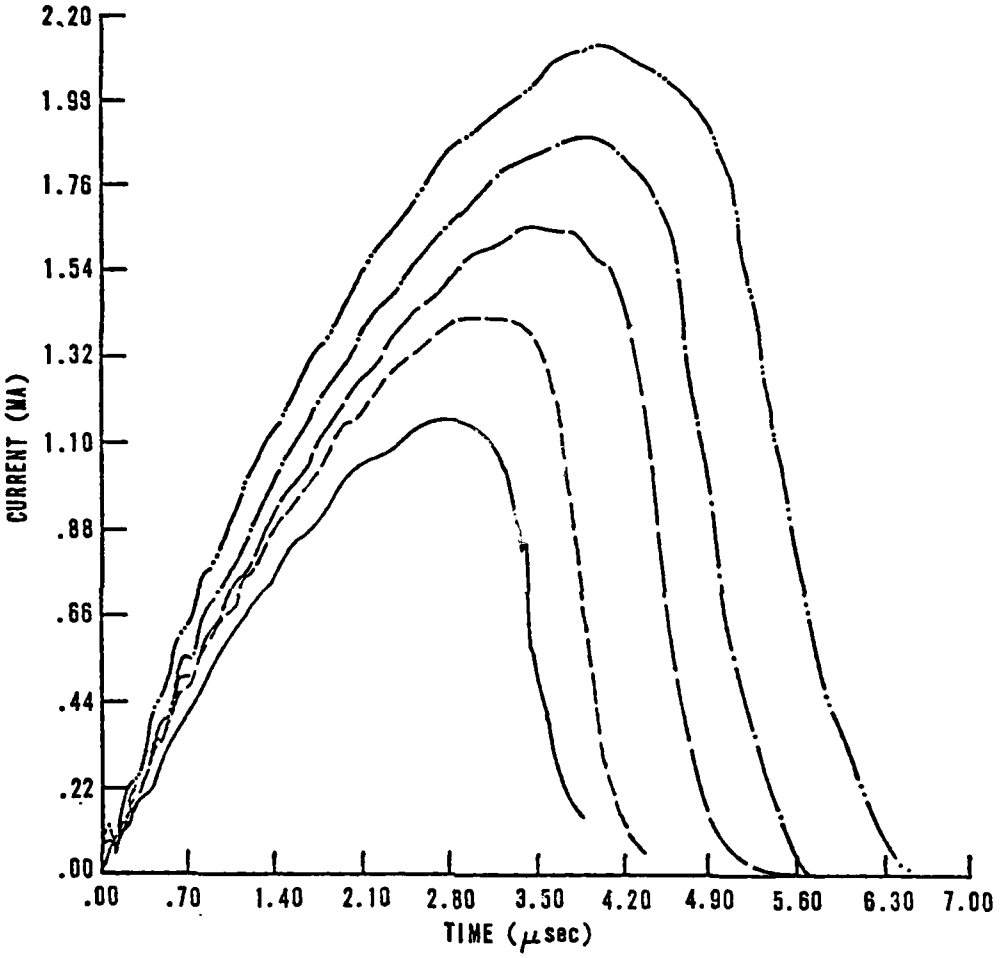

Figure 7. Current Data for Approximately 25-g Copper Foil Fuses. (Same sizes as for figure 6.)

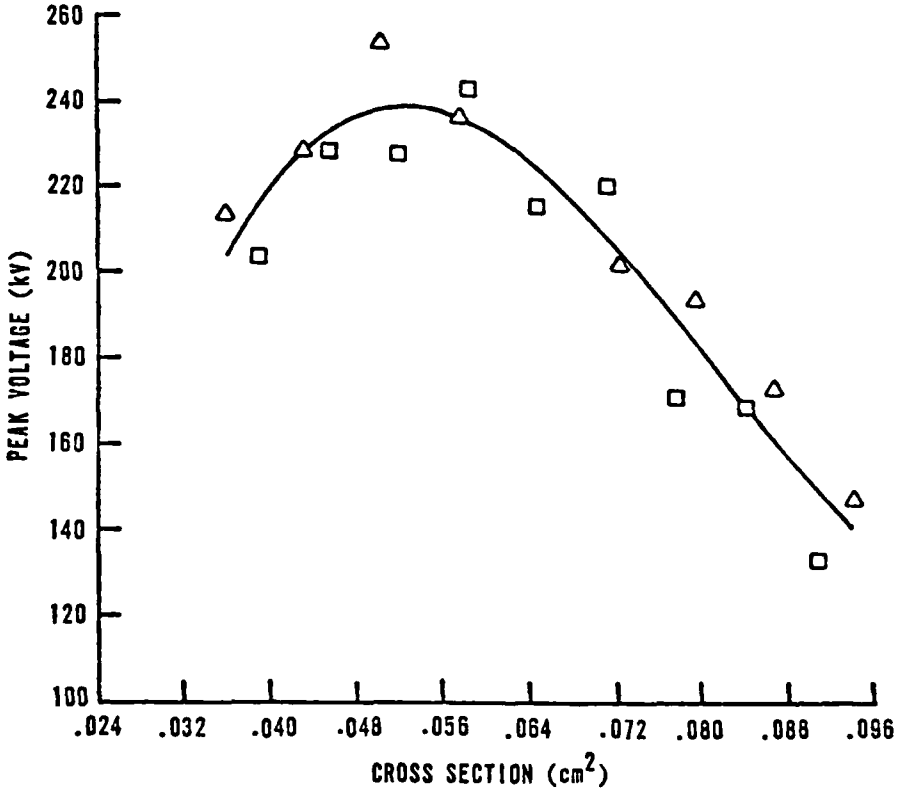

Figure 8. Peak Fuse Voltage Plotted Against Foil Cross Section.
(△: constant foil mass fuses
□: constant inductance fuses
The line is a cubic least-squares fit to all the points.)

shows the peak voltage plotted against the cross-sectional area. The solid line is a cubic least-squares fit to the points. Clearly, a single curve can reasonably fit the data for both families of fuses. A Maisonnier-size fuse, with an inductance of 14 nH for the bank configuration used here, would have a cross-sectional area of 0.078 cm^2.

Data in figures 9 and 10 are the voltage and current traces for two fuses of equal length and cross-sectional area, and, therefore, mass of copper. The difference is that one was split into halves which were separated in space. A 46.6-cm-long by 27.1-cm-wide foil was split lengthwise into two equal pieces. These were then attached to the fuse clamp on the bank in the usual way. The inside edges of the two pieces were separated by 18.7 cm. This set of two parallel fuses was then fired.

A comparison of the data in figures 9 and 10 show that the split foil fused substantially earlier, and reached significantly higher peak voltage and current. The difference in inductance between the split and normal fuses is calculated to be slightly less than 1 nH, which is less than 2% of the total system inductance. Therefore, the inductance difference alone cannot explain the differerence in performance.

A further test was made by splitting a fuse and then putting the two halves together with no space between them. This resulted in a shot that was not significantly different from the single-piece fuses of the same size. These tests are taken to indicate that edge effects are very important to the fuse behavior, which is not surprising since the current density is known to be higher at the edges of parallel plate transmission lines than at the center.

Voltage oscillations on the early time data for the split fuse were unique to that particular configuration. However, they were present on all of the two-piece fuses that were fired. These oscillations were not present on the three- and four-piece fuses that were fired.

Figures 11 and 12 compare the two-piece and four-piece fuses. Total cross-sectional area and length of the foils were the same: 0.065 cm^2 and 46.6 cm, respectively. Aside from the early time oscillations, there is no significant difference in fuse behavior.

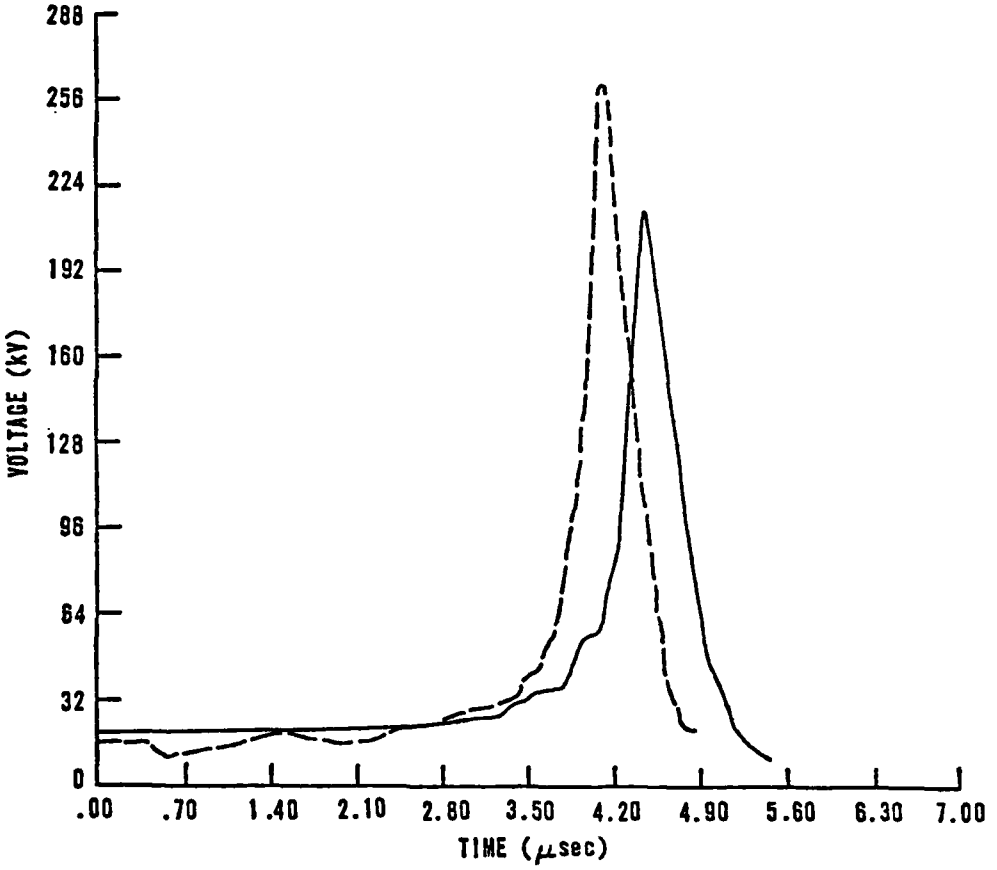

Figure 9. Comparison of the Voltage Data for One-Piece and Two-Piece Fuses. (Solid line: one-piece fuse; dashed line: two-piece fuse. Both fuses were 46.6 cm long and have a cross-sectional area of 0.065 cm^2.)

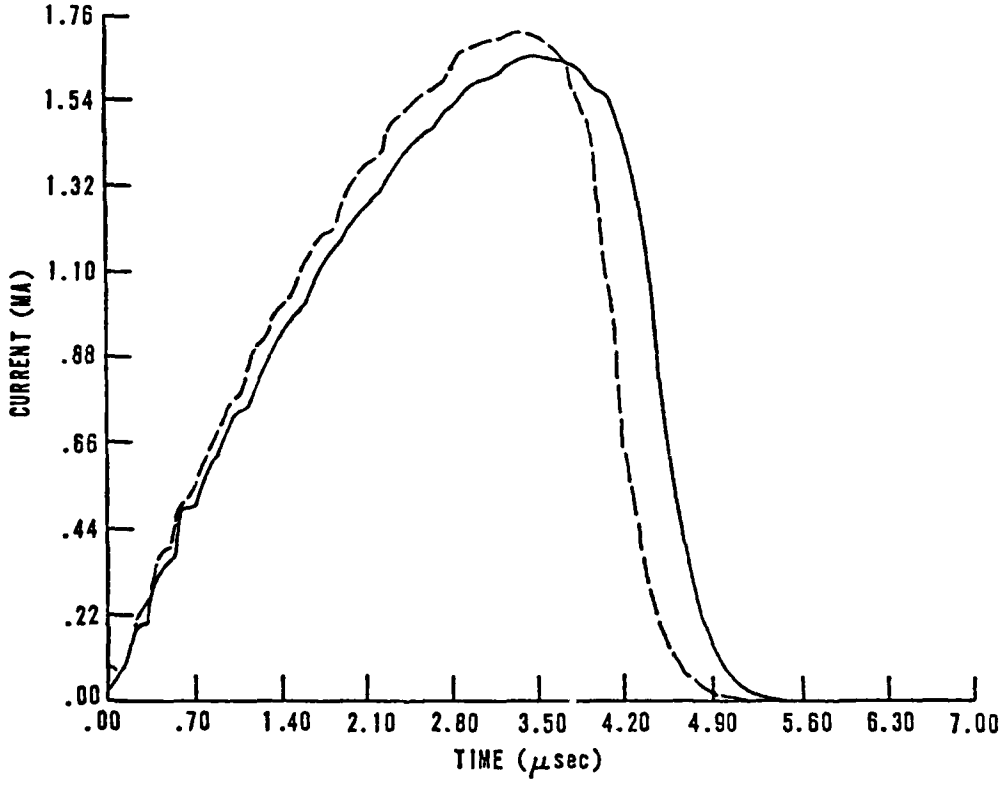

Figure 10. Comparison of the Current Data for One-Piece and Two-Piece Fuses. (Rest of caption same as for figure 9.)

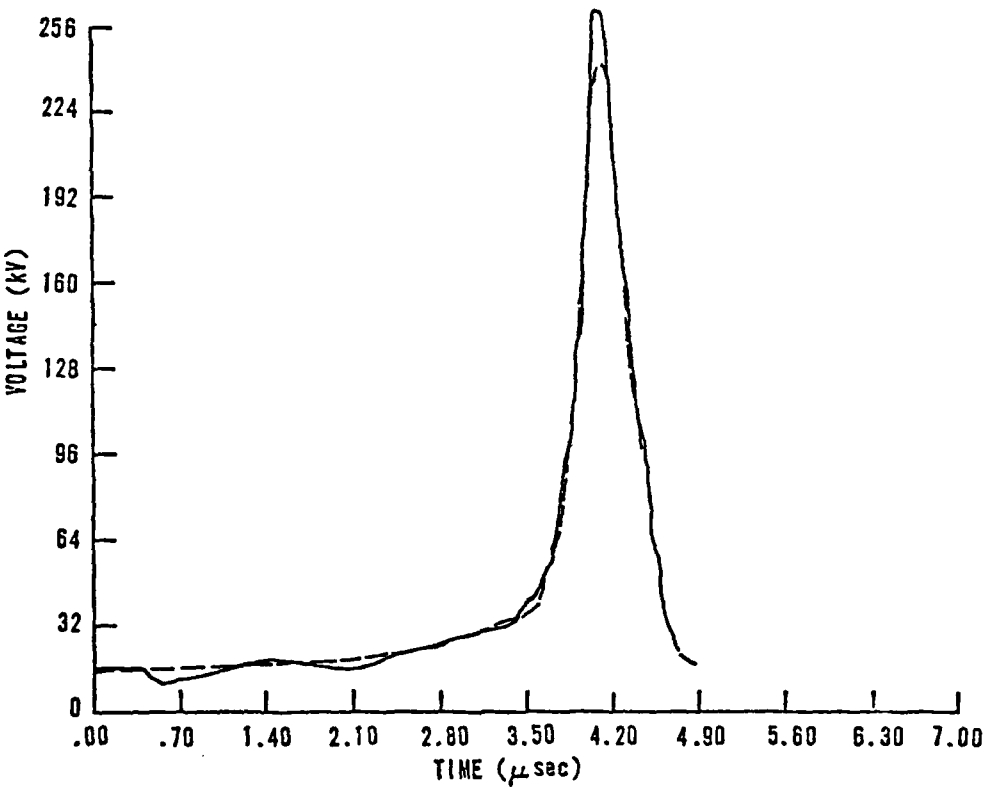

Figure 11. Comparison of the Voltage Data for Two-Piece and Four-Piece Fuses. (Solid line: two-piece fuse; dashed line: four-piece fuse. Both fuses were 46.6 cm long and had a cross-sectional area of 0.065 cm^2.)

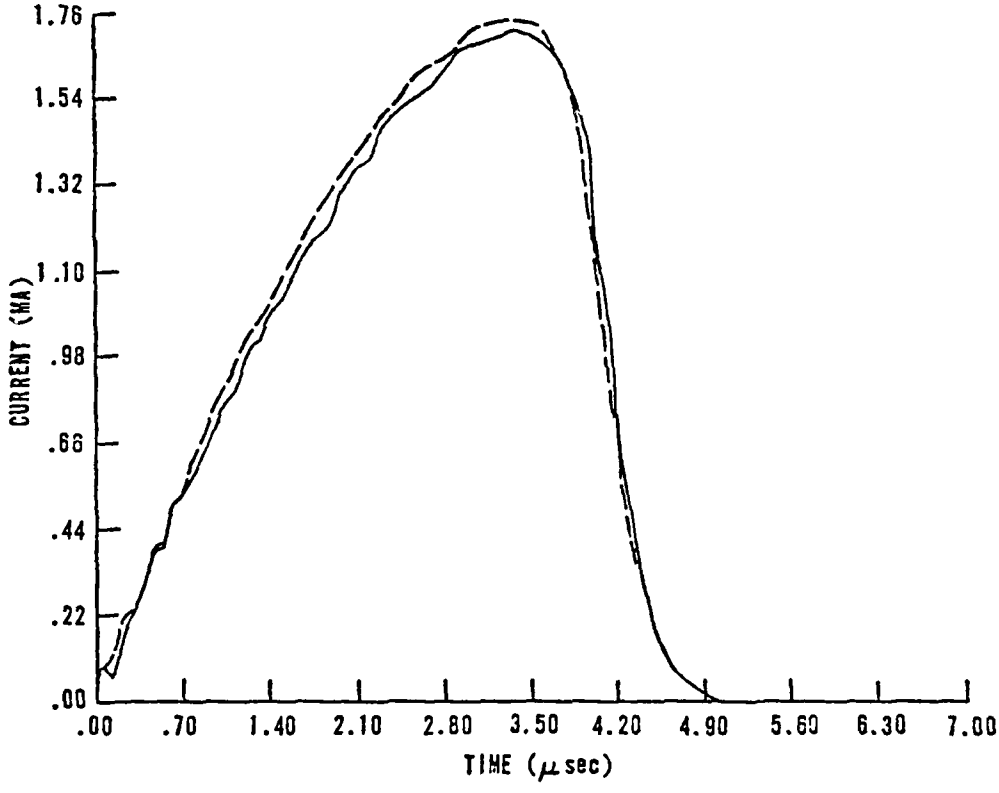

Figure 12. Comparison of the Current Data for Two-Piece and Four-Piece Fuses. (Rest of caption same as for figure 11.)

There was 6.3-cm separation between each of the fuse elements in the four-piece fuse. Consequently, both fuse packages had an overall width of about 46 cm. Perhaps this is the important parameter; nevertheless, it was not investigated.

In order to check the overall reproducibility of the data, the last fuse fired was the same size as the first one. Figures 13 and 14 compare the results of these two fuses. There is a significant difference; nevertheless, the differences are much less than those between different fuse sizes (c.p. figures 4-7). Even splitting the fuse is much more significant. It is felt that the differences arise from differences between the copper at the beginning and the end of the roll.

Instantaneous fuse resistance can be calculated using the equation

$$R_F(t) = \frac{V_F(t) - L_F\dot{I}(t)}{I(t)} \tag{1}$$

where V_F is the fuse voltage, L_F is the fuse inductance, I is the current, and $\dot{I}$ is the time rate of change of the current. A quantity that has units of resistivity can be defined by

$$\rho(t) \equiv R_F(t)\ \frac{s}{\ell} \tag{2}$$

where s is the initial cross-sectional area of the fuse and ℓ is the length. Clearly, ρ is the average resistivity of the fuse material if the foil dimensions have not changed. Henceforth, ρ will be treated as though it were the resistivity of the copper.

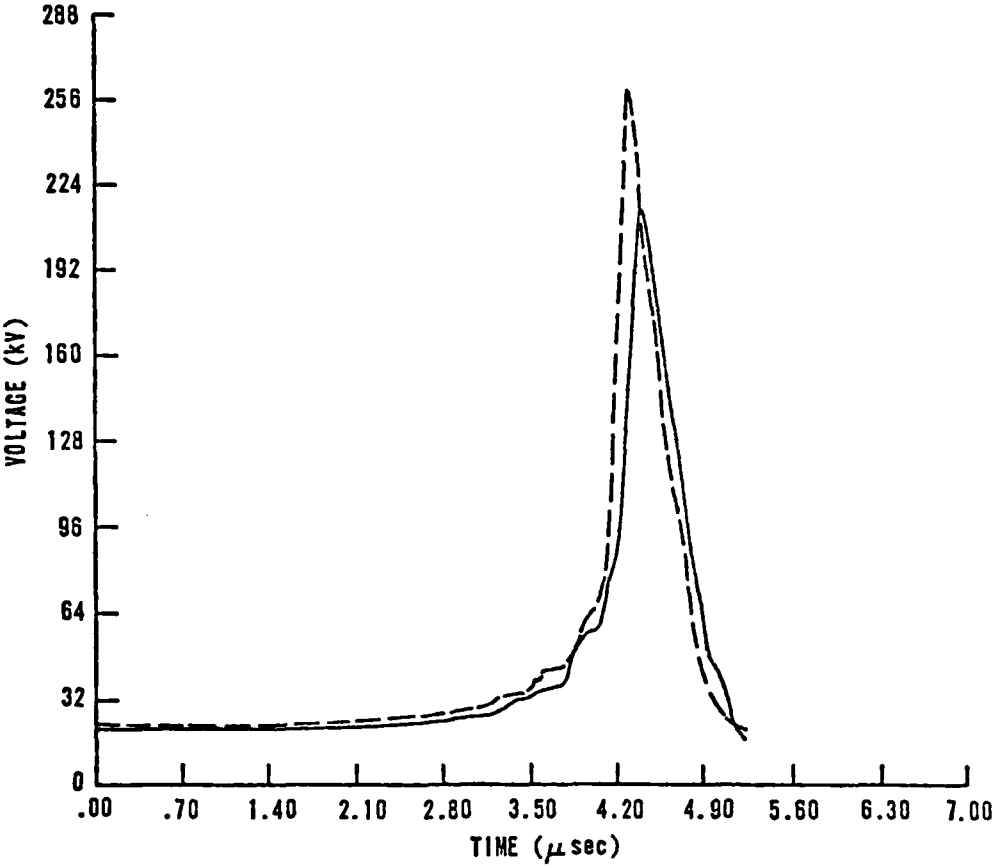

Figure 13. Comparison of the Voltage Data for Fuses Fired Early (Solid Line) and Late (Dashed Line) in the Experimental Program. (Both fuses were 46.6 cm long and 27.1 cm wide. Approximately 5 months and 50 shots separated these two.)

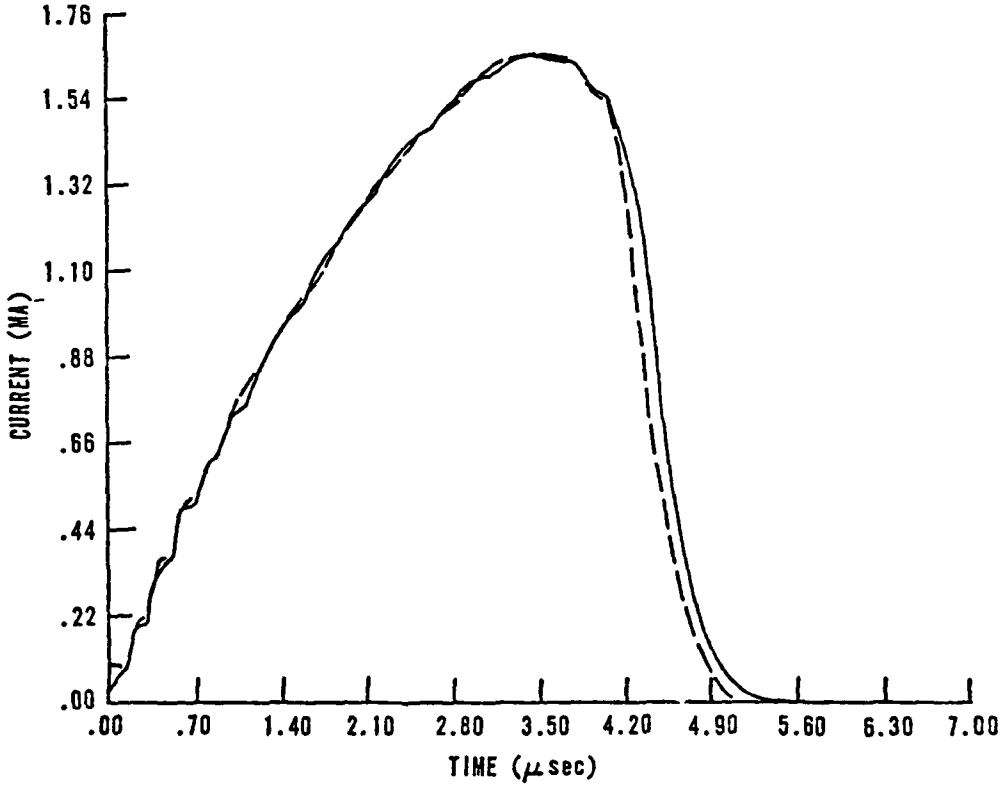

Figure 14. Comparison of the Current Data for Fuses Fired Early (Solid Line) and Late (Dashed Line) in the Experimental Program. (Rest of caption same as for figure 13.)

Resistivity is plotted as a function of specific energy absorbed by the fuse material in figure 15 for five different fuses of the constant inductance family. Specific energy is defined by

$$\mathcal{E}(t) \equiv \frac{1}{\gamma} \int_0^t \rho(t') J^2(t') \, dt' \tag{3}$$

where

$$J(t) = \frac{I(t)}{s} \tag{4}$$

and γ is the mass density of copper (8.96 g/cm^3, reference 9).

Several features of these curves are worth noting. As the peak current density increases, the specific energy at which the resistivity starts to climb steeply increases. Moreover, the climb is steeper for lower peak current density. Particularly for high current-density fuses, there is evidence of a plateau in the resistivity versus specific energy curve. This plateau is at a higher resisitivity for lower current densities. Similar results have been reported for exploding copper wires (reference 10).

Resistivity of the same fuses is plotted against specific action in figure 16. Specific action is defined by

$$G(t) \equiv \int_0^t J(t')^2 \, dt' \tag{5}$$

The specific action at which the resistivity climbs steeply is seen to be a function of current density. Nevertheless, the dependence is somewhat weaker.

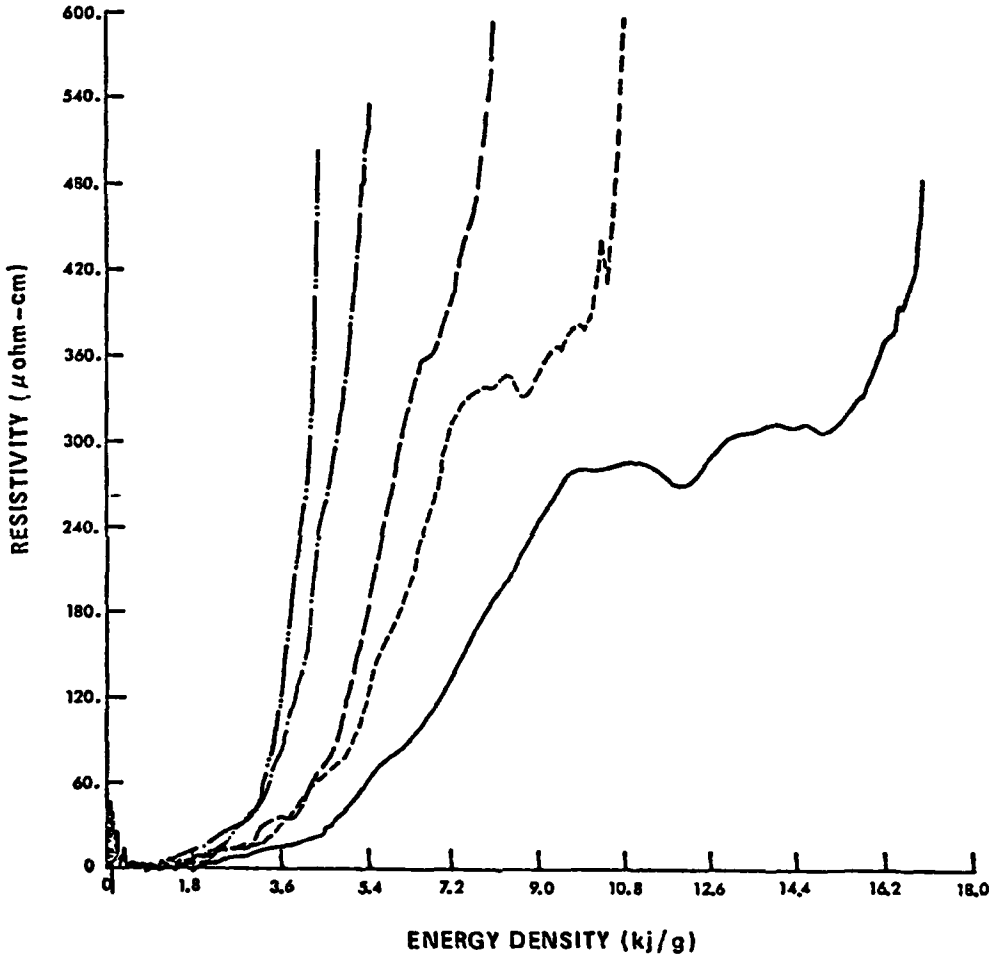

Figure 15. Resistivity Plotted Against Specific Energy Absorbed for Five Fuses of the Constant Inductance Family. (Solid: 27.9 cm long by 16.3 cm wide; dashed: 37.2 cm long by 21.7 cm wide; long dash: 46.6 cm long by 27.1 cm wide; dot-dash: 55.9 cm long by 32.5 cm wide; and double dot-dash: 65.2 cm long by 38.0 cm wide.)

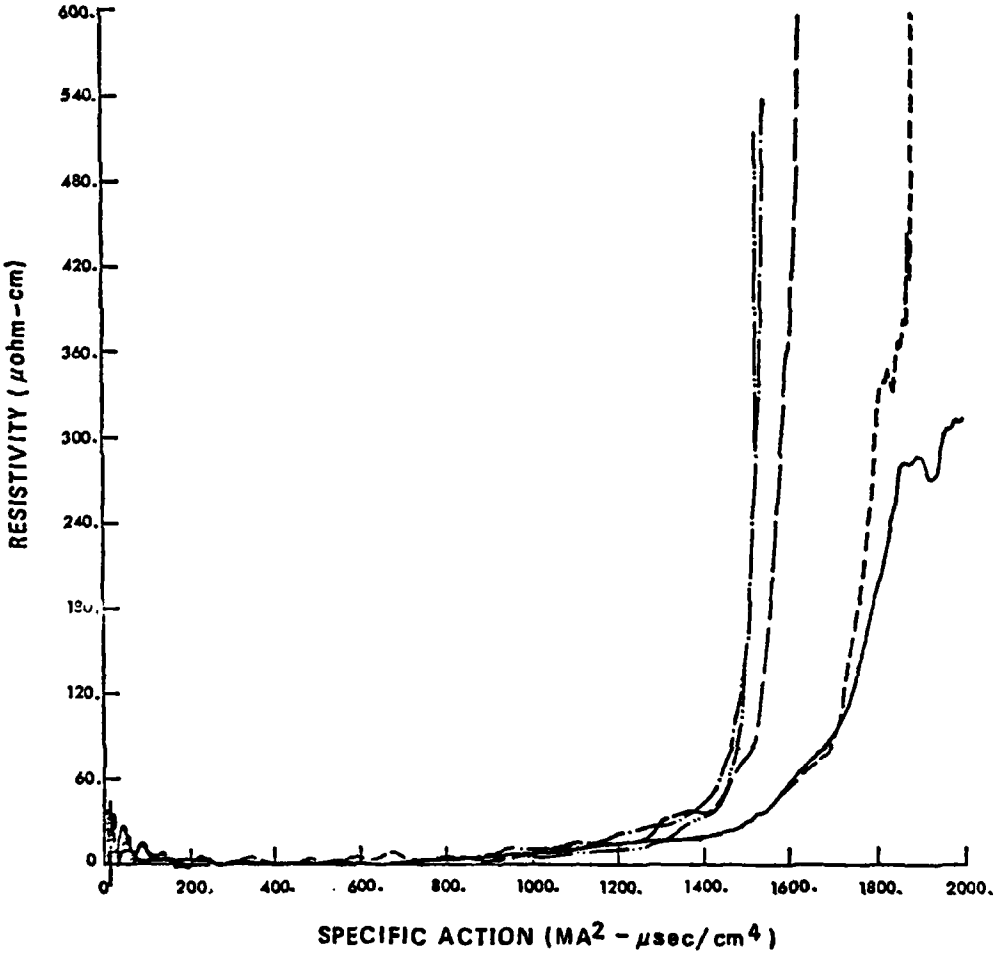

Figure 16. Resistivity Plotted Against Specific Action for Five Fuses of the Constant Inductance Family. (Rest of caption same as for figure 15.)

SECTION IV

RESISTIVITY MODEL

In general the resistivity versus energy density curves for the fuses within each family can be ordered by the peak current density. That is, the foil that reaches a higher peak current density fuses at a higher specific energy. If fuses from the constant mass family are compared to the fuses from the constant inductance family, this ordering is no longer possible.

Figure 17 shows the resistivity versus specific energy curves for three fuses. Of the three fuses, one belonged to the constant inductance family, one belonged to the constant mass family, and one belonged to both families. These three fuses reached peak densities of 30.3, 28.3, and 25.6 MA/cm^2, respectively. Clearly, these curves cannot be ordered on the basis of peak current density.

Figure 18 shows the resistivity versus specific action curves for the same three fuses. These curves can be ordered on the basis of peak current density. When all of the data are compared, the ordering is no longer perfect. Nevertheless, it is much better than trying to order the resistivity versus specific energy curves.

It is tempting to try to find a simple dependence of the burst specific action on current density. (Burst specific action is defined as that specific action at which the copper has completely vaporized.) In other words, is there a parameter of the fused circuit behavior, G_e, such that resistivity as a function of G_e can be uniquely defined without an explicit dependence on J? We call G_e the effective specific action and define it like specific action with the addition of an implicit functional dependence on J called F(J)

$$G_e(t) = \int_0^t J^2(t')\, F(J(t'))\, dt' \qquad (6)$$

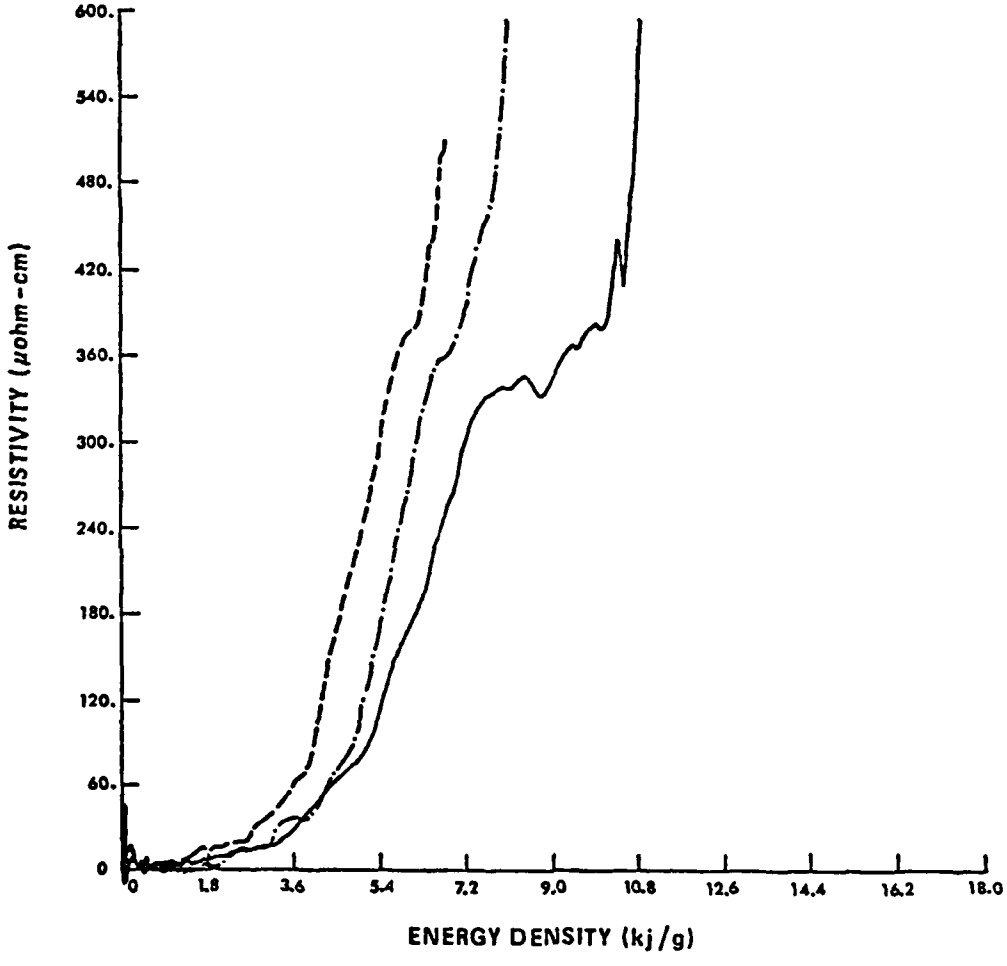

Figure 17. Resistivity Plotted Against Specific Energy for Three Fuses. (Solid line: 37.2 cm long by 21.7 cm wide, 14 nH, 17.3 g of copper, 30.3 MA/cm^2 peak current density; dashed line: 57.7 cm long by 21.0 cm wide, 23 nH, 25.9 g of copper, 28.3 MA/cm^2 peak current density; dot-dash: 46.6 cm long by 27.1 cm wide, 15 nH, 27 g of copper, 25.6 MA/cm^2 peak current density.)

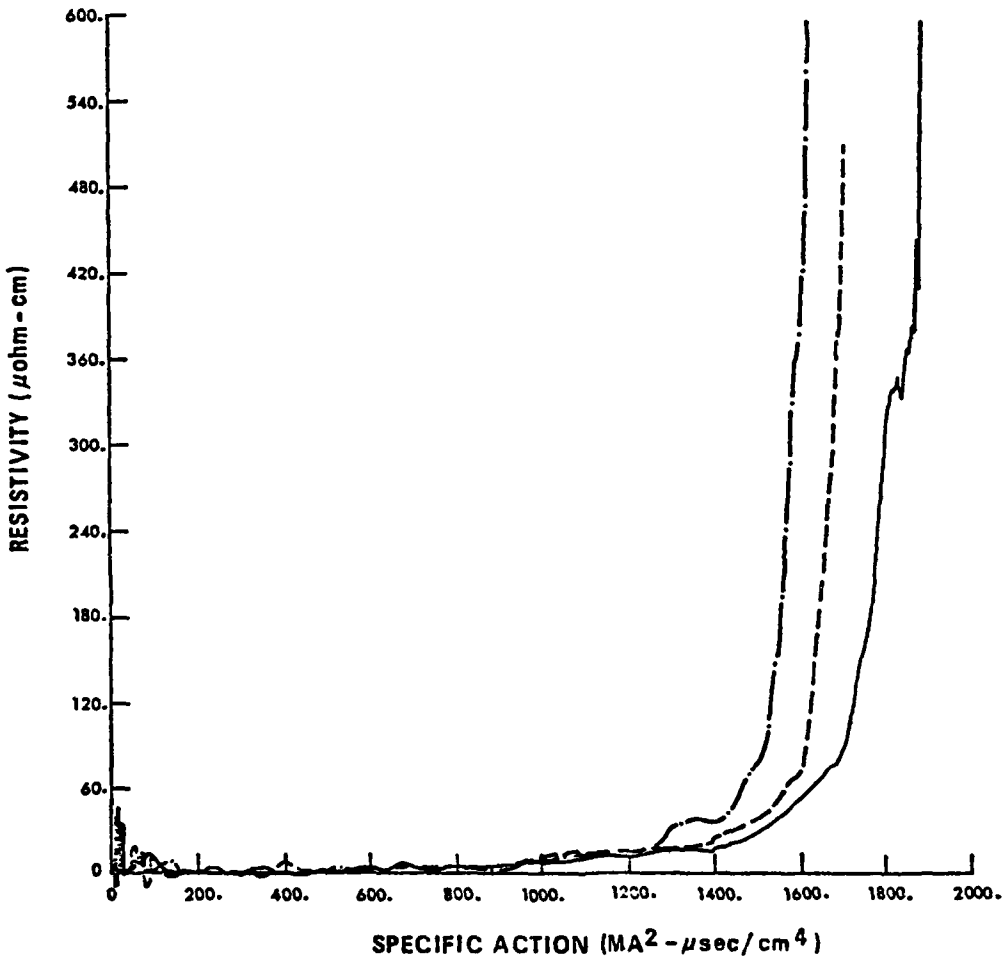

Figure 18. Resistivity Plotted Against Specific Action for Three Fuses. (Rest of caption same as for figure 17.)

The function F(J) is a correction factor that must be employed when using some resistivity function. T. J. Tucker and R. P. Toth have published resistivity versus specific action curves for many materials (reference 11). These data were taken at constant current densities, and they are ideal as a basis for a resistivity model.

The problem now is to find the function F(J), such as that at the time of peak voltage,

$$G_e\left(t_B\right) = G_o = \text{constant} \tag{7}$$

for all the fuses. Several different functional forms were tried. The form that was both simple and did a good job in fitting the data is the linear form

$$F(J) = 1 + A\left(J - J_o\right) \tag{8}$$

A and J_o are to be taken from fits to the data.

Tucker reports the peak in the resistivity curve for copper to occur at 1730 $MA^2-\mu s/cm^4$. Using this to be the effective specific action at which copper bursts, a fit to the data presented here leads to the values for A and J_o shown in table 1.

TABLE 1

RESISTIVITY MODEL CONSTANTS

G_o*	1730 $MA^2-\mu s/cm^4$
A	$-0.0236\ cm^2/MA$
J_o	$25.7\ MA/cm^2$

*Reference 11.

The resistivity versus specific action curve is steeper when the foils fuse at lower specific actions. Exactly how to do this with a model is a problem, if the model consists of a data table. Therefore, it was decided to fit a curve to Tucker's data. The curve that was chosen consists of the sum of eight gaussian functions. The centroids, heights, and full widths at half maximum (FWHM) are listed in table 2.

TABLE 2

PARAMETERS FOR THE FIT TO TUCKER'S DATA*

Center (MA^2-$\mu s/cm^4$)	Height ($\mu\Omega$-cm)	FWHM (MA^2-$\mu s/cm^4$)
6589	3707	3994
1733	516.1	66.9
966	4.8	93.6
1084	2.9	181.2
1588	8.5	73.2
1594	10.2	28.6
1825	56.6	116.9

*Reference 11.

As the foil fuses at smaller values of specific action, the rise becomes steeper, and the plateau in the resistivity occurs at higher values. This can be accomplished with a gaussian by increasing the amplitude and decreasing the FWHM. It was decided to change the amplitude and FWHM by the same ratio; that is, the area under each gaussian in the fit was kept constant. A reasonable fit to the data was obtained by miltiplying the amplitude of each gaussian by the factor

$$1 + 1.2\left(1 - \frac{G}{G_e}\right) \tag{9}$$

where G is the specific action and G_e is the effective specific action. The FWHM are then divided by this factor.

Copper vapor from the fuse quickly condenses on the glass beads inside the fuse package. Therefore, the fuse normally does not restrike, and the resistance remains high. In order to model this, the resistivity is kept constant after the effective specific action has reached 1734 MA^2-$\mu s/cm^4$.

Predicted resistivity as a function of specific action is plotted for three current densities in figure 19. These curves were made using the model described above, assuming constant current densities. Since the highest current density obtained in the present data was about 35 MA/cm^2, it is unwise to extrapolate this resistivity model much beyond that level. The resistivity curves in figure 19 show regions where the resistivity is decreasing. This is an artifact of the way in which the shape of the resistivity curve is modified and it is a shortcoming of this resistivity model.

In order to see how well the use of the effective specific action as the independent variable removes the current density dependence from the resistivity, compare figures 20 and 21. Resistivity is plotted as a function of specific action in figure 20 for three fuse sizes. Resistivity is plotted as a function of effective specific action for the same three fuses in figure 21. The upper end of each curve corresponds to peak voltage in that fuse.

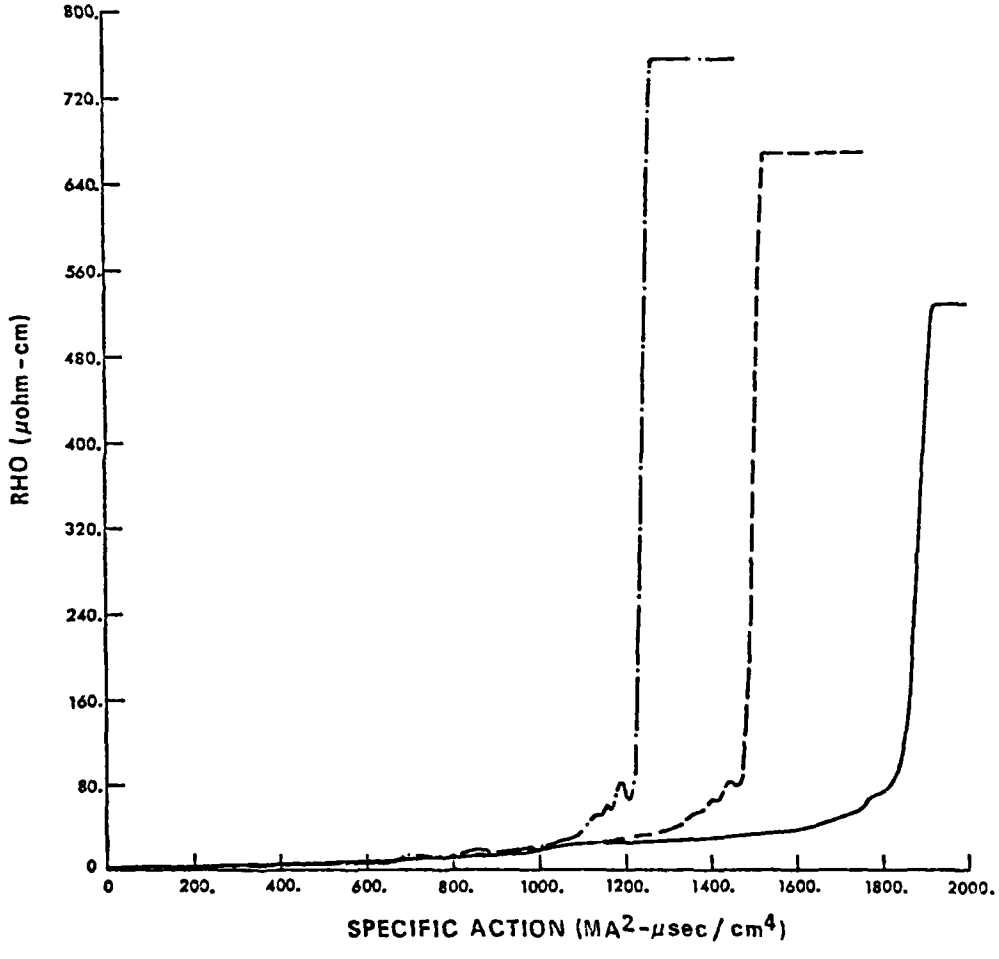

Figure 19. Model Predictions for Resistivity Versus Specific Action at Three Current Densities. (Solid: 30 MA/cm^2; dash: 20 MA/cm^2; dot-dash: 10 MA/cm^2.)

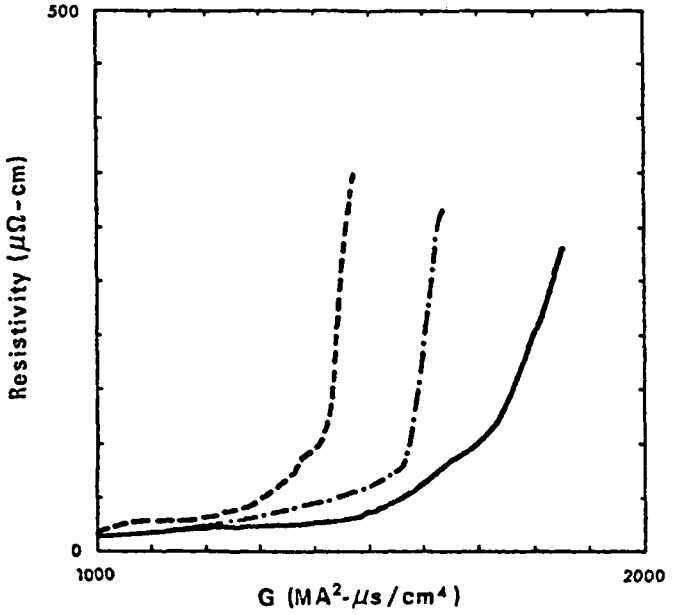

Figure 20. Plot of Resistivity Versus Specific Action for Three Fuses. (Solid line: 27.9 cm long by 16.3 cm wide; dashed line: 31.7 cm long by 36.3 cm wide; dot-dashed line: 41.9 cm long by 24.4 cm wide.)

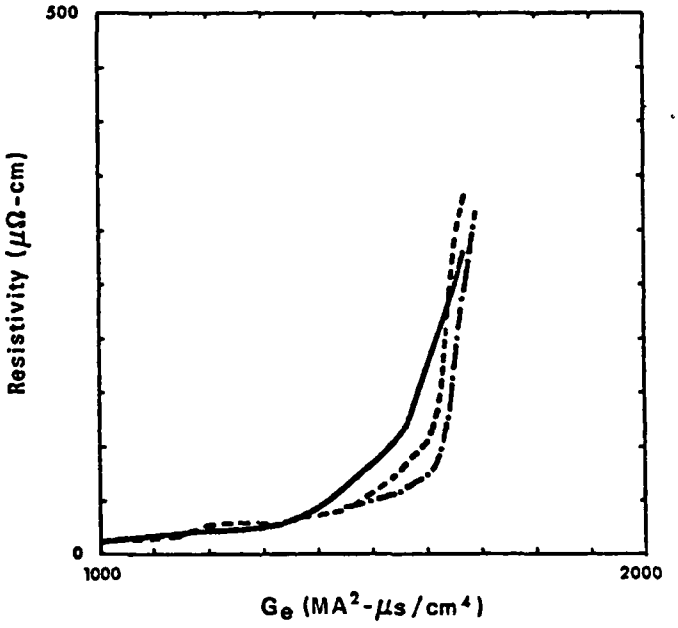

Figure 21. Plot of Resistivity Versus Effective Specific Action for Three Fuses. (Rest of caption same as for figure 20.)

SECTION V

FUSE CODE AND COMPARISONS WITH EXPERIMENT

A computer code was written to simulate the performance of copper foil fuses. The resistivity model described in the previous section is built into the code. This code has been used to predict the behavior of a wide range of fuse sizes with generally good results.

Since edge effects are important to fuse behavior, some two-dimensional effects are explicitly treated. In the code, the fuse is considered to be a number of parallel copper ribbons with the edge of one touching the edge of the next, and all connected in parallel to the bank. Typically, the fuse is thought of as consisting of 100 ribbons. Mutual inductances are calculated and the ribbons interact magnetically, but current is not allowed to transfer from within one ribbon to another.

It is assumed that there is the same voltage drop around each loop containing a ribbon. At any given time, therefore, this voltage is given by

$$\mathcal{E} = R_i I_i + L_i \dot{I}_i + \sum_{k \neq i} M_{ik} \dot{I}_k \tag{10}$$

where R_i, L_i, I_i, and $\dot{I}_i$ are the resistance, self inductance, current, and time rate of charge of current in the $\underline{i}$th ribbon, M_{ik} is the mutual inductance between ribbons i and k, and $\dot{I}_k$ is the time rate of change of current in the $\underline{k}$th ribbon. If we define $L_i = M_{ii}$, then this equation becomes

$$\mathcal{E} = R_i I_i + \sum_{k} M_{ik} \dot{I}_k \tag{11}$$

There are, of course, N equations, where N is the total number of loops. The external circuit equation is

$$\frac{1}{C} Q = R_x I + L_x \dot{I} + \mathcal{E} \tag{12}$$

where C is the bank capacitance, Q is the charge on the bank, R_x and L_x are the external circuit resistance and inductance, respectively, I is the total current and $\dot{I}$ is the time rate of change of total current. Combining these two equations results in a set of N simultaneous linear differential equations that must be solved.

These simultaneous equations compose an Nth order matrix equation, which is solved for the $\dot{I}_i$ at a succession of time steps. At each time step the Q, I, and I_i are calculated from the previous values of Q, I, I_i, and $\dot{I}_i$. Then the present values of $\dot{I}_i$ are calculated. The resistivity model is used to calculate the R_i at each time step. This procedure is repeated until the problem is finished. Time step size is varied to ensure that $\dot{I}$ changes only by a small amount in each time step. More detailed information on the code can be found in reference 12.

Simulations were run for all of the foil sizes used, including split foils. Figure 22 is a comparison between the simulations and experiments for four different fuse sizes. It can be seen that the simulations range from rather good to only fair.

In all cases, the initial voltage of the simulation is lower than the experiment. However, this difference does not have the same ratio for all the foil sizes. Therefore, it is not the result of a simple calibration error in the voltage probe.

A curve was least square fit to the dI/dt data of each fuse shot. Inductance was calculated from the intercept of each curve and the calculated fuse inductance subtracted. The bank inductance was calculated by averaging these numbers to be 44 $\pm$ 3 nH. Therefore, fuse inductance calculations are not in error by enough to account for this discrepancy.

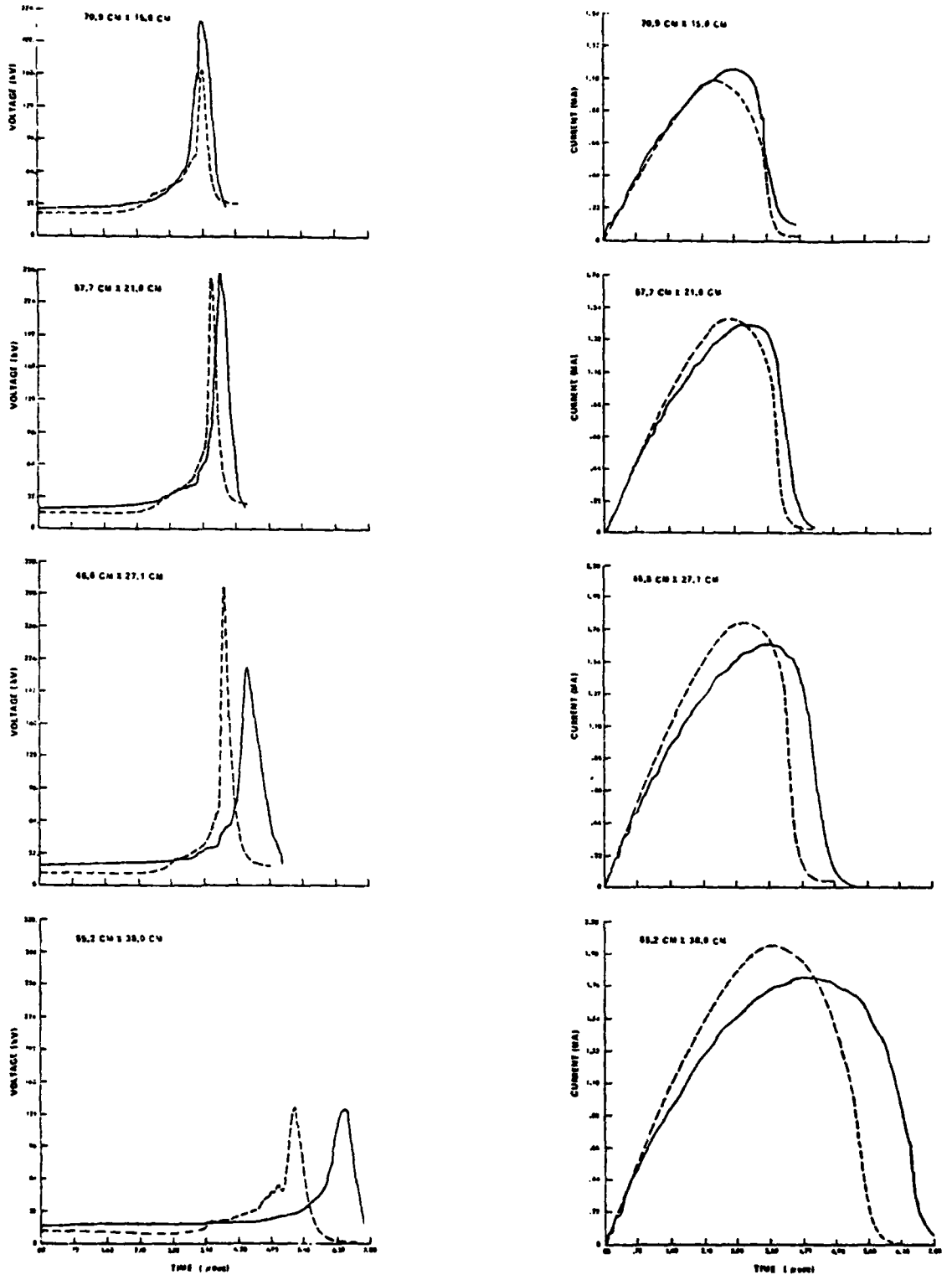

Figure 22. Comparison of Computer Simulations with Experimental Results for Four Fuse Sizes. (Solid lines: experiment; dashed lines: simulations.)

Figure 23 compares fuse voltage curves near peak voltage for two simulations. The solid curve is for a normal one-piece fuse, while the dashed line is for a split fuse. There is a difference between the two curves; nevertheless, it is very small compared to the experimental difference (c.p. figure 9).

Although the fuse code does predict qualitative fuse behavior, it does not make predictions that are as accurate as one would like. It is felt that the reason for this is that two-dimensional effects are very important, that is, significant current can flow perpendicular to the length of the fuse. The present fuse code does not allow for these currents. Perhaps a code such as PLATE (reference 13) or EBFI (reference 14) with the present resistivity model would be more successful.

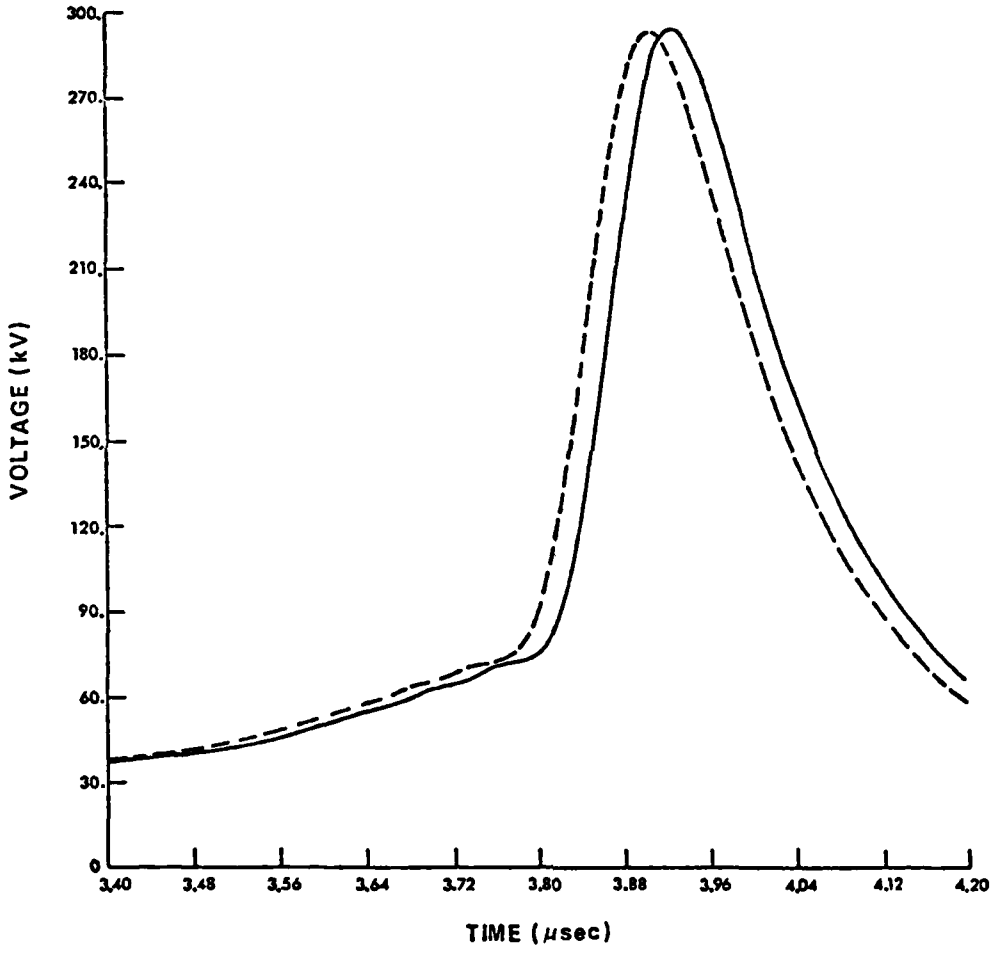

Figure 23. Comparison of Computer Simulation Voltage Pulses for One-Piece and Two-Piece Copper Foil Fuses. (Both foils are 46.6 cm long with a cross-sectional area of 0.065 cm^2.)

SECTION VI

CHOICE OF FUSE SIZE

In order to select the fuse size that is appropriate for a given capacitor bank, we adopt the first of Maisonnier's criteria. That is, the fuse should burst at peak current (reference 3). Furthermore, it is assumed that before the foil bursts, its resistance is negligible and that the current density is uniform everywhere in foil.

Under these circumstances, the current waveform will be

$$I = V_o C \omega \sin \omega t \tag{13}$$

where C and V_o are the bank capacitance and initial charge voltage, and

$$\omega = (LC)^{-1/2} \tag{14}$$

where L is the total inductance. The condition for burst at peak current is

$$G_o = G_e = \int_o^{\pi/2\omega} J^2\left(1 + A\left(J - J_o\right)\right) dt \tag{15}$$

where G_o, A, and J_o are constants and J is the current density. Substituting I/s for J and integrating, gives

$$G_o = \left(1 - AJ_o\right) \frac{V_o^2 C}{\omega L} \frac{\pi}{4} \frac{1}{s^2} + A \frac{V_o^3 C^2}{L} \frac{2}{3} \frac{1}{s^3} \tag{16}$$

Multiplying by $\frac{s^3}{G_o}$ and collecting the terms give

$$s^3 - \frac{1 - AJ_o}{G_o} \frac{\pi}{4} \frac{V_o^2 C}{\omega L} s - \frac{2}{3} \frac{A}{G_o} \frac{V_o^3 C^2}{L} = 0 \tag{17}$$

If there were no dependence of the burst specific action on the current density, then A would be 0. Solving equation (17) for s with A = 0 gives

$$s = \sqrt{\frac{\pi}{4G_o}} \frac{V_o C}{(LC)^{1/4}} \tag{18}$$

Maisonnier's equation for the cross-sectional area of the fuse can be written in the form

$$s = \frac{1}{\sqrt{2^{3/2} k_1 a}} \frac{V_o C}{(LC)^{1/4}} \tag{19}$$

where k and a are parameters that are defined in reference 3. By comparing equations (18) and (19), we can make the identification

$$2^{3/2} k \; a = \frac{4G_o}{\pi} \tag{20}$$

Using the value 5.9×10^{16} for a (reference 4), gives $k_1 = 1.4$. Di Marco and Burkhardt found that a value of about 2 gave a good fit to their data (reference 4).

The present data indicates that the burst specific action is a function of current density and A is not 0. Defining

$$\alpha \equiv -\frac{1 - AJ_o}{G_o} \; \frac{\pi}{4} \; \frac{V_o^2 C}{\omega L} \tag{21}$$

and

$$b \equiv -\frac{2}{3} \frac{A}{G_o} \; \frac{V_o^3 C^2}{L} \tag{22}$$

the cubic equation

$$s^3 + \alpha s + b = 0 \tag{23}$$

results.

If $b^2/4 + a^3/27 > 0$, there will be only one real solution to equation (23). Conversely, if it is less than 0, there will be three real roots. The dividing line between these two cases occurs when

$$0 = \frac{b^2}{4} + \frac{a^3}{27} = \frac{A^2 V_o^6 C^4}{9 G_o^2 L^2} - \frac{\left(1 - AJ_o\right)^3 \pi^3 V_o C}{1728 G_o^3 \omega L^2} \tag{24}$$

This can be reduced to

$$\omega = \frac{\pi^3 \left(1 - AJ_o\right)^3}{192 G_o A^2} = 6.95 \times 10^5 \ s^{-1} \tag{25}$$

This corresponds to a quarter-cycle time of 2.26 μs.

If the natural risetime of the bank is slower than this, there will be three real solutions. They are

$$s = \sqrt{\frac{\pi\left(1 - AJ_o\right)}{3G_o}} \; \frac{V_o C}{\sqrt[4]{LC}} \; \cos\left(\frac{\phi}{3} + n\frac{2\pi}{3}\right) \tag{26}$$

where n = 0,1,2. The angle ϕ is defined by

$$\cos\phi = -\sqrt{\frac{192 G_o A^2}{\pi^3 \left(1 - AJ_o\right)^3}} \; \frac{1}{\sqrt[4]{LC}} \tag{27}$$

Clearly, Q will always be greater than $\pi/2$ and less than π. Therefore, $\frac{\phi}{3}$ will always be greater than $\pi/6$ and less than $\pi/3$, and there will always be two positive real solutions for s. For example, if L = 60 nH and C = 158 μF, ϕ = 2.32 rad, and the three solutions for s are 0.100 cm^2, -0.135 cm^2, and 0.035 cm^2. A comparison with figure 8 shows that the two positive roots bracket the experimental fuses.

If the assumption of zero resistance until the foil fuses were strictly valid, the fuses with cross-sectional areas 0.100 and 0.035 cm^2 would reach peak current densities of 25.7 and 73.5 MA/cm^2, respectively. As presented here, F(J) becomes negative above 68 MA/cm^2. This means that for the smaller positive root, $G_e(t)$ is not monotonic. In fact, $G_e(t)$ increases to values larger than G_o and then decreases until its final value is G_o. This is clearly unphysical, since the foil would fuse the first time $G_e(t)$ reached G_o. Indeed this is what happens experimentally. Consequently only one of the roots is physically meaningful.

If the risetime of the bank is faster than 2.26 μs, there is only one real root to equation (23), and it is

$$s = \left[\sqrt[3]{\frac{2}{3} + \sqrt{1 - \frac{\pi^3\left(1 - AJ_o\right)^3}{192 G_o A^2} \sqrt{LC}}} \right.$$

$$\left. + \sqrt[3]{\frac{2}{3} - \sqrt{1 - \frac{\pi^3\left(1 - AJ_o\right)^3}{192 G_o A^2} \sqrt{LC}}} \right]$$

$$\times \sqrt[3]{\frac{A}{G_o}} \frac{V_o C}{\sqrt[3]{LC}} \qquad (28)$$

Since A/G_o is negative, s will always be negative.

Clearly, there is little meaning to the solution of equation (23) for fast rise banks.

In order for the correction factor F(J) to be valid, J must not greatly exceed the maximum value of J that was encountered in the experiments from which F(J) was inferred. That is, J must not greatly exceed 35 MA/cm^2. Equations (13) and (26) can be used to infer the peak current density

$$J_{pk} = \frac{\sqrt{\frac{3G_o}{\pi(1 - AJ_o)}}}{\sqrt[4]{LC}\cos\frac{\phi}{3}} \tag{29}$$

If the risetime is 3 μs,

$$J_{pk} = 36 \text{ MA/cm}^2 \tag{30}$$

Moreover, if the risetime is longer than 3 μs, the peak current density will be smaller than 36 MA/cm^2. Therefore, the optimum fuse cross-sectional area can be predicted if the risetime is longer than about 3 μs. This can be expected to be somewhat better than Maisonnier's equation, because it takes the current density dependence of the fuse behavior into account.

In order to select the length of the fuse, one more criterion must be specified. Since the fuse resistivity plateaus, it is convenient to choose the shut-off time τ.

Then the current in the fuse will decay in a time characteristic of L/R, where L is the total inductance and R is the plateau resistance of the fuse. Therefore, the length is specified by

$$\ell = \frac{Ls}{\rho_o \tau} \tag{31}$$

where ρ_o is the plateau resistivity.

A reasonable value for the plateau resistivity is 300 $\mu\Omega$-cm (figure 15). If one chooses τ to be 300 ns, L is 60 nH, and s is 0.065 cm^2, then

$$\ell = 43 \text{ cm} \tag{32}$$

This is very close to the 0.065 cm^2 by 46.6 cm fuse that was chosen using Maisonnier's energy dissipation criterion (reference 3). Notice, however, that one can choose a wide range of lengths to select the desired shut-off time without regard to the amount of energy being absorbed.

SECTION VII

CONCLUSION

Copper foils have been successfully used as fuses on a 200-kj capacitor bank. While no parallel load was switched into the circuit, the current in the fuse was shut off at rates as high as 4×10^{12} A/s. Voltage pulses with a full width at half maximum of about 300 ns and peaks at 4 μs into the discharge have been observed. Therefore, ratios of conduction time to turn-off time in excess of 10 have been observed.

Resistivity as a function of specific action and current density has been inferred. In general, a higher peak current density results in fusing at a higher specific action. The current density dependence has the effect of extending the range of foil sizes which will work as fuses.

Postulating that the foil should reach burst specific action at peak current leads to a method of determining the optimum cross-sectional area. If the burst specific action is assumed to be independent of the current density, the resulting relation is the same as that derived by Maisonnier. On the other hand, if the current density dependence inferred from the present data is employed, a different equation is applicable fuse size. This inferred optimum size is valid so long as the peak current density does not greatly exceed 35 MA/cm^2. This is equivalent to specifying that the quarter cycle risetime of the bank is 3 μs or greater. Since the current density dependence was included in the derivation of the present technique for selecting the fuse cross-sectional area, it should be more appropriate in the region where it is valid than that of Maisonnier.

Choosing the optimum fuse length is largely subjective. The data presented here indicate that the fuse material will absorb large amounts of energy without restriking. Moreover, the foil will still effectively fuse at relatively low specific energy. Therefore, it is suggested that the fuse length be chosen to give the desired current turn-off time.

In light of the large range of specific energy which a fuse will absorb and still function, perhaps it is not necessary to totally vaporize the fuse material. Possibly all that is necessary is to liquify the material and drive it rapidly into the glass beads. Further work would be necessary in order to address this question.

ACKNOWLEDGMENTS

The authors would like to thank R. E. Reinowsky, W. L. Baker, G. F. Kiuttu, and M. C. Clark for many helpful discussions and suggestions, and T. J. Tucker for supplying the resistivity data.

REFERENCES

1. Janes, G. S. and H. Koritz, Rev. Sci. Instrum. 30, p. 1032 (1959).

2. Early, H. C. and F. J. Martin, Rev. Sci. Instrum. 36, p. 1000 (1965).

3. Maisonnier, C., J. G. Linhart, and C. Gourlan, Rev. Sci. Instrum. 37, p. 1380 (1966).

4. Di Marco, J. N. and L. C. Burkhardt, J. Appl. Phys. 41, p. 3894 (1970).

5. Baker, W. L., M. C. Clark, J. H. Degnan, G. F. Kiuttu, C. R. McClenahan, and R. E. Reinovsky, Journal of Applied Physics 49, 4694 (1978).

6. Robson, A. E., P. Turchi, W. Lupton, M. Ury, and W. Warnick, "A Multi-Megajoule Inertial-Inductive Energy Storage System," Proceedings of the International Conference on Energy Storage, Compression, Switching , Asti-Torino, Italy, November 5-7, 1974, W. H. Bostick, V. Nardi, O. S. F. Zucker, Eds., 1976.

7. Megagauss Magnetic Field Generation by Explosives and Related Experiments, EUR2750.e, edited by H. Knoepfel and F. Herlach (EURATOM, Brussels, 1966).

8. Di Marco, J. N., private communication.

9. Hammond, C. R., Handbook of Chemistry and Physics, R. W. Weast, Ed., Chemical Rubber Co., Cleveland, OH, 47 edition (B-108), 1966.

10. Webb, F. H., Jr., H. H. Hilton, P. H. Levine, and A. T. Follestrump, Exploding Wires, W. G. Chace and H. K. Moore, Eds., Plenum Press, Inc., NY, V. II (37), 1962.

11. Tucker, T. J. and R. P. Toth, Sandia Laboratories, Albuquerque, NM, Report No. SAND-75-0041, 1975.

12. McClenahan, C. R. , FUSE: A Quasi Two-Dimensional Fuse Code, Air Force Weapons Laboratory, Kirtland AFB, NM Technical Report (to be published).

13. Justice, J. A., PLATE: A 2-D Transmission Line Current Symmetry Code, Air Force Weapons Laboratory, Kirtland AFB, NM, Report No. AFWL-TR-76-205, 1976.

References (continued)

14. Logan, J. D. and R. S. Lee, EBFI: A Computer Simulation of the Preburst Behavior of Electrically Heated Exploding Foils, Lawrence Livermore Laboratory, Livermore, CA, Report No. UCRL-52003, 1976.


FILMED
7
8